
Unified Text-to-Image Generation and Retrieval

Leigang Qu¹ Haochuan Li¹ Tan Wang^{2*} Wenjie Wang^{1*} Yongqi Li³
Liqiang Nie⁴ Tat-Seng Chua¹

¹National University of Singapore ²Nanyang Technological University

³Hong Kong Polytechnic University ⁴Harbin Institute of Technology (Shenzhen)

{leigangqu, wenjiawang96, nieliqiang, liyongqi0}@gmail.com

haochuan@u.nus.edu tan317@ntu.edu.sg dcscts@nus.edu.sg

<https://tiger-t2i.github.io>

Abstract

How humans can efficiently and effectively acquire images has always been a perennial question. A typical solution is *text-to-image retrieval* from an existing database given the text query; however, the limited database typically lacks creativity. By contrast, recent breakthroughs in *text-to-image generation* have made it possible to produce fancy and diverse visual content, but it faces challenges in synthesizing knowledge-intensive images. In this work, we rethink the relationship between text-to-image generation and retrieval and propose a *unified* framework in the context of Multimodal Large Language Models (MLLMs). Specifically, we first explore the intrinsic discriminative abilities of MLLMs and introduce a generative retrieval method to perform retrieval in a training-free manner. Subsequently, we unify generation and retrieval in an autoregressive generation way and propose an autonomous decision module to choose the best-matched one between generated and retrieved images as the response to the text query. Additionally, we construct a benchmark called TIGeR-Bench, including creative and knowledge-intensive domains, to standardize the evaluation of unified text-to-image generation and retrieval. Extensive experimental results on TIGeR-Bench and two retrieval benchmarks, *i.e.*, Flickr30K and MS-COCO, demonstrate the superiority and effectiveness of our proposed method.

1 Introduction

The explosion of visual information on the Web significantly challenges human information access. Text-to-Image Retrieval (T2I-R) [31, 46, 69] is one of the main channels to efficiently obtain visual information given a text query. However, T2I-R is limited to retrieving existing images in the database, lacking flexibility and creativity. Recent years have witnessed thrilling progress in Text-to-Image Generation (T2I-G) [43, 47, 50], which directly generates new images to satisfy human’s visual information needs. However, T2I-G falls short of handling knowledge-intensive concepts, *e.g.*, landmarks and natural species, leading to the hallucination problem [19, 22]. In this light, a single T2I-R or T2I-G model may not satisfy diverse and evolving human information needs. It is pivotal to unify both T2I-R and T2I-G within a framework for visual information delivery.

To this end, a straightforward solution is to empower discriminative models with the generation ability. However, the early-stage trial (*e.g.*, JEM [15]) requires extra generative training and may compromise the original discriminative power. Another recent attempt [4, 29] is to adapt generative diffusion models [43] to achieve discriminative tasks. Despite the significance, these methods are limited to diffusion models and inevitably suffer from the notorious inefficiency problem caused by

*Corresponding Author: Tan Wang and Wenjie Wang

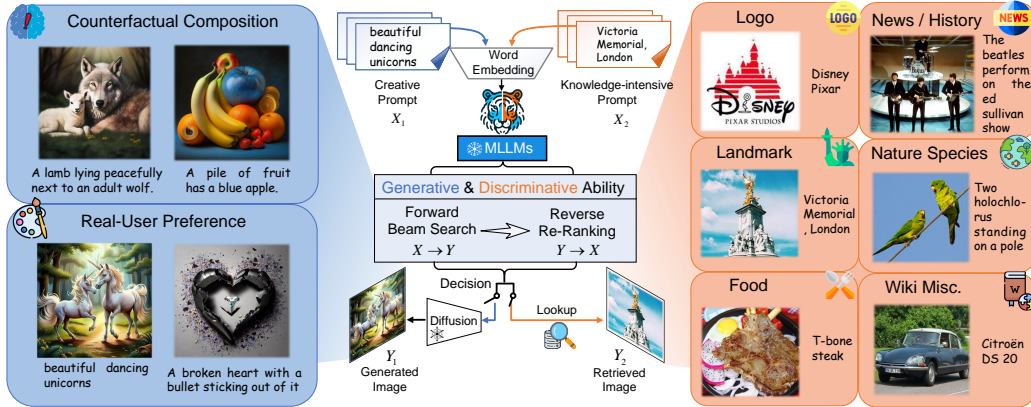


Figure 1: We consider both **creative** domains and **knowledge-intensive** domains for general image acquisition towards unified Text-to-Image Generation and Retrieval (TIGeR), and build the TIGeR-Bench including 8 domains for the unified comprehensive evaluation.

iterative denoising [18]. Moreover, diffusion models are usually tailored for simple discriminative tasks such as image classification [16, 29] and it is difficult for diffusion models to process complex human intentions for large-scale retrieval in practical scenarios [52].

Different from diffusion models, Multimodal Large Language Models (MLLMs) offer another form of generative paradigm to solve broad vision-language problems, garnering significant attention for their powerful intention understanding and instruction following abilities [42, 57]. Recently, notable efforts [7, 14, 54, 55, 64] incorporate MLLMs with external T2I-G models [43, 50] for image synthesis. Nevertheless, these works only consider T2I-G without T2I-R. Even though GILL [24] fuses an LLM and the image encoder & decoder to achieve the unified ability of generation and retrieval, it highly depends on an external retriever (*i.e.*, CLIP [46]) for the discriminative ranking in the dedicated embedding space. As such, the inefficiency problem [56, 72] of the dense retrieval paradigm still hinders large-scale image retrieval of GILL.

In this work, we propose to elegantly unify Text-to-Image Generation and Retrieval (**TIGeR**) within MLLMs, a promising task to achieve more flexible image acquisition, as shown in Fig. 1. To this end, we first delve into the intrinsic bidirectional (*i.e.*, text-to-image and image-to-text) discriminative abilities of MLLMs in Sec. 3.2. Specifically, we study the potential of bidirectional conditional likelihoods as the proxies of semantic similarity by assessing the performance in image-text matching. Based on the discriminative abilities, we present an efficient generative retrieval method with forward beam search and reverse re-ranking as in Sec. 3.3, unifying both T2I-R and T2I-G in an autoregressive generation manner. Besides, we propose an autonomous decision mechanism to adaptively choose one from retrieved and generated images according to user prompts. To comprehensively evaluate the performance of MLLMs on TIGeR, we build a benchmark (**TIGeR-Bench**) in Sec. 4 from two aspects, one for creative images from the counterfactual world or users’ imaginative prompts [23], and the other is derived from six knowledge-intensive domains (*e.g.*, news, landmark, and natural species). Additionally, we carry out extensive experiments to assess the TIGeR performance of representative MLLMs, verifying the effectiveness of the proposed method. Overall, we summarize the contributions into three points.

- Driven by diverse and complex practical scenarios for visual information access, we propose to unify text-to-image generation and retrieval in the context of MLLMs.
- We comprehensively inspect the intrinsic cross-modal discriminative abilities of MLLMs and propose a training-free generative retrieval approach based on bidirectional discrimination, thus unifying text-to-image generation and retrieval in an autoregressive generation manner. And we present an autonomous decision mechanism to adaptively select retrieved or generated images.
- We construct a comprehensive image acquisition benchmark, including creative and knowledge-intensive domains, to evaluate the TIGeR performance of existing MLLMs. Extensive experiments on TIGeR-Bench and two T2I-G benchmarks including Flickr30K [68] and MSCOCO [35] verify the effectiveness of the proposed framework.

2 Related Work

Text-to-Image Generation. T2I-G has aroused wide attention in both academia and industry over the past decade, with advancements ranging from Generative Adversarial Networks [49] to Auto-regression Models [6, 70] and Diffusion Probabilistic Models (DPMs) [5, 18]. Recent breakthroughs in DPMs, guided by the scaling law [21, 30], have propelled T2I-G to new heights, *e.g.*, models like DALL-E 2 [47] and DALL-E 3 [1], the Imagen series [51], and the Stable Diffusion (SD) series [9, 43, 50]. Concurrently, efforts have been made to enhance composed text-image alignment [3, 12, 45, 67] and cater to human preference [26, 65, 66]. However, prior works predominantly focus on creative domains for image generation, neglecting the imperative of knowledge-intensive image acquisition tailored to human needs.

Multimodal Information Retrieval. Early studies on multimodal information retrieval focused on feature representation [11, 33] and modality interaction [27, 44] for precise cross-modal similarity estimation. Recent advancements, propelled by large-scale pre-training, have led to improved retrieval performance and generalization in vision-language models [8, 32, 46]. More recently, researchers have explored more challenging scenarios, such as fine-grained interaction [36], equivariant similarity [61], multimodal instruction following [62], and chat-based IR [28]. Despite thrilling progress, retrieval systems are inherently limited by database size, and incapable of creating new visual content.

Multimodal Large Language Models. Empowered by the versatility and flexibility of LLMs, pioneering works on MLLMs have shown impressive understanding capabilities [39, 75]. Recent research explores image generation through two categories: 1) *Continuous Visual Representation* methods aim to align visual representations from LLMs with condition embeddings of SD through regression [7, 24, 54, 64, 76] or score distillation [7] objectives. 2) *Discrete Visual Tokenization* methods [14, 14, 40, 71] first encode an image into a sequence of discrete codes [10, 14, 20, 58], and then employ next-token prediction to train MLLMs. To synthesize images, the discrete codes are decoded into the pixel space via VQ-GAN or SD. In this work, we resort to the discrete paradigm to be consistent with the inherent discreteness of language. Compared with the existing work, our TIGeR method achieves comprehensive image acquisition, encompassing both content creation and knowledge retrieval within a unified framework.

3 Methodology

In this section, we first formulate the unified problem in Sec. 3.1, and then explore the intrinsic cross-model discriminative ability of MLLMs for semantic similarity measurement in Sec. 3.2. Based on the ability, we propose a unified framework, as shown in Fig. 2, including generative retrieval in Sec. 3.3, synchronous generation and retrieval, and decision-making in Sec. 3.4.

3.1 Problem Formulation

The goal of this work is to satisfy complex human visual information needs by acquiring images from diverse domains in a unified MLLM framework. We formulate this problem autoregressively:

$$p(Y|X) = \prod_{i=1}^N p(y_i|Y_{<i}, X), \quad (1)$$

where X denotes a textual prompt provided by humans, tokenized into a sequence $X = [x_1, \dots, x_M]$. $Y = [y_1, \dots, y_N]$ denotes the sequence of visual tokens that can be decoded into an image, with $Y_{<i}$ referring to the tokens before i -step. By sampling from the conditional distribution, we obtain a sequence instance, *i.e.*, $Y^* \sim p(Y|X)$, where $Y^* \in \mathbb{V}^N$ and \mathbb{V} denotes the visual token space defined by a visual vocabulary, and $|\mathbb{V}| = V$ is the vocabulary size. \mathbb{V}^N denotes the Cartesian product of N token spaces, *i.e.*, the whole discrete visual space. To achieve unified generation and retrieval, an MLLM is required to possess the following three capabilities:

- **Creativity** to generate novel photorealistic images by sampling from $p(Y|X)$,
- **Discrimination** to match vision and language and retrieve the relevant images from an image database or gallery \mathcal{G} ,
- **Decision** to automatically determine the superior option between generation and retrieval.

Considering the proficiency of recent MLLMs [7, 14, 74] in creative text-to-image generation, we will focus on exploring the discriminative ability for text-to-image retrieval and unified generation and retrieval with decision-making in the following.

3.2 Intrinsic Discriminative Ability of MLLMs

For effective text-to-image retrieval, LLMs should possess a strong discriminative ability which is fundamental for accurate semantic similarity estimation between the prompt and images in the database. To probe such intrinsic capability, we will introduce three training-free proxies as follows.

To estimate the semantic similarity $s(X, Y)$ between a given text prompt/query X and an image Y , a straightforward approach is to employ the conditional likelihood based on autoregressive factorization as the proxy:

$$s(X, Y) = \log p(Y|X) = \sum_{i=1}^N \log p(y_i|Y_{<i}, X), \quad (2)$$

where $p(Y|X)$ denotes the likelihood of an image $Y \in \mathcal{G}$ from the database conditioned on the given prompt X . In practice, we can attain it by computing the cross entropy between the predicted logits and the image tokens. However, we observed this proxy performs weakly in practice, as shown in Tab. 1. Similar phenomena also happened in recent studies [25, 37] for diffusion and captioning models.

We attribute this problem to the *modality bias*, including the visual bias for T2I-G models and the linguistic bias for image captioning models, respectively. In this study, the visual bias largely stems from the unbalanced distribution, *i.e.*, $p(Y)$, and thus we introduce an alternative proxy as,

$$s(X, Y) = \log \frac{p(Y|X)}{p(Y)^\eta} = \sum_{i=1}^N \log p(y_i|Y_{<i}, X) - \eta \sum_{i=1}^N \log p(y_i|Y_{<i}), \quad (3)$$

where we use the visual prior $p(Y)$ to help debiasing with a strength factor η , which can be estimated by $p(Y|\bar{X})$. \bar{X} refers to a special prompt without any descriptive content, *e.g.*, a null character or “Can you give me an image?”.

In addition to the debiasing strategy, we propose another option to circumvent the unbalanced prior distribution. Different from the generation process without the image Y , the retrieval task allows the model to access all images in the database, which means we can estimate the semantic similarity in a reverse way by predicting the conditional likelihood of another modality, *i.e.*, X , with:

$$s(X, Y) = \log p(X|Y) = \sum_{i=1}^M \log p(x_i|X_{<i}, Y). \quad (4)$$

To perform this reverse calculation, we view MLLMs as image captioners.

The above three training-free proxies of semantic similarities could be calculated in parallel because all tokens have been accessible beforehand. After calculating the similarities between the given textual prompt and all images from the database, we could sort them to attain the ranking list. Compared with the prior work GILL [24], this method is seamlessly integrated with generative pre-training, eliminating the need for additional discriminative training, such as contrastive learning, and benefits from fine-grained cross-modal interaction within MLLMs.

3.3 MLLMs-based Generative Retrieval

The above proxies make it possible to calculate cross-modal similarities and carry out ranking based on which. However, it is inefficient since the requirement of $|\mathcal{G}|$ times of forward propagation of MLLMs, each time with the extensive parameterization and the intricate attention interaction. To tackle this issue and achieve an optimal balance between efficiency and recall, we introduce forward beam search and reverse re-ranking, as shown in Fig. 2.

Table 1: Text-to-image ranking performance of three similarity (Sim.) proxies for SEED-LLaMA [14] and LaVIT [20] on MS-COCO [35].

Sim. Proxy	SEED-LLaMA		LaVIT	
	R@1	R@5	R@1	R@5
Random	0.02	0.10	0.02	0.10
$\log p(Y X)$	3.50	8.79	0.02	0.16
$\log \frac{p(Y X)}{p(Y)}$	26.25	54.57	23.43	48.52
$\log p(X Y)$	49.34	75.45	50.35	70.87

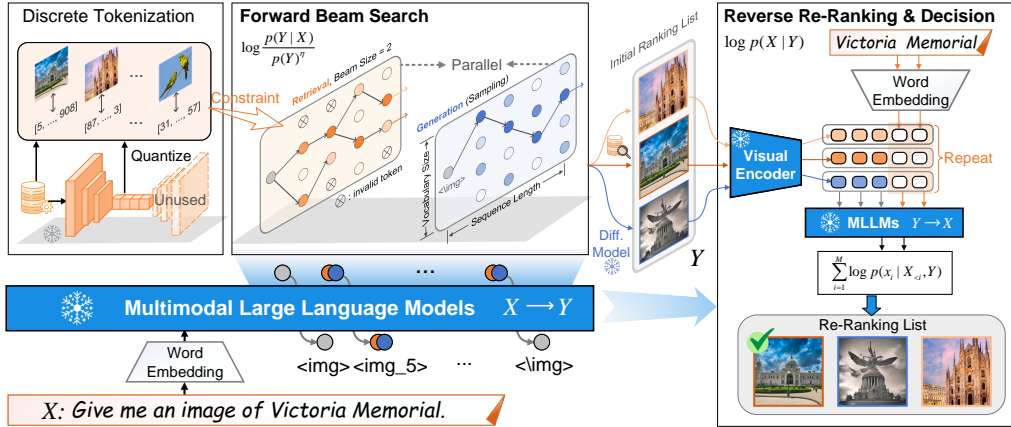


Figure 2: Overview of the framework to unify text-to-image generation and retrieval. Images from the database are first tokenized into discrete codes and a lookup table is maintained for the correspondence between discrete codes and images. The given prompt X is first fed into a MLLM and Forward Beam Search is performed to retrieve and generate images in parallel. The prompt and obtained images are then fed into the same MLLM for Reverse Re-Ranking and Decision-making.

Forward Beam Search. Inspired by the advancement of generative retrieval [34, 56], we adopt constraint generation via autoregressive token decoding and beam search [13] with the beam size B to recall a fixed number of images. Specifically, we compress all images in the database into discrete tokens and store them in a Trie structure. This Trie structure constrains the sampling space and ensures that the generated prefix at any timestep corresponds to at least one image in the database. Once the beam search is finished, we could obtain a ranking list of B sequences of visual tokens, each of which corresponds to an image in the database. This process aims to obtain a list of images given the prompt, thus the direction has to be $X \rightarrow Y$, which means we can only adopt the two forward proxies illustrated in Eqn. 2 or Eqn. 3. However, the forward beam search method could significantly improve the efficiency since it only requires $N(N \ll |\mathcal{G}|)$ times of forward propagation of MLLMs. N denotes the length of the visual token sequence for an image.

Reverse Re-Ranking. Despite the improved efficiency, the semantic matching accuracy of the two forward proxies is obviously weaker than that of the reverse one in Eqn. 4, as shown in Tab. 1. Given the ranking list $\mathcal{R} = [Y_1, \dots, Y_B]$ obtained by forward beam search, we resort to the reverse proxy in Eqn. 4 for re-ranking and attain the final ranking list \mathcal{R}^* .

3.4 Unifying Generation and Retrieval

The discrete visual tokenization strategy enables MLLMs to generate both language and visual content in an autoregressive generation manner. The proposed forward beam search in Sec. 3.3 performs retrieval by autoregressively generating visual tokens one by one. Naturally, we can unify generation and retrieval based on MLLMs under the same autoregression framework and make a decision between the generated and retrieved images to meet complex real-world requirements.

Synchronous Generation and Retrieval. In this unified framework, MLLMs can synchronously conduct unconstrained and constrained token decoding for image generation and retrieval, respectively. As shown in Fig. 2, these two tasks can be performed in parallel by maintaining respective search paths, which also requires N times of forward propagation. Each path corresponds to a sequence of discrete visual tokens. We can generate a new image Y^G by a diffusion decoder conditioned on the sequence, and meanwhile, immediately find the retrieved top-1² image Y^R via the lookup table.

Decision Making. Given the generated image Y^G and the retrieved image Y^R , we choose the better one based on the intrinsic discriminative abilities of MLLMs, as discussed in Sec. 3.3. Specifically, we calculate two semantic similarities $s(X, Y^G)$ and $s(X, Y^R)$ using the three proxies mentioned

²This work only considers one generated image and the top-1 retrieved image, but the proposed framework can also acquire more than one images and choose the best one.

Table 2: Performance comparison on TIGeR-Bench. “Token” refers to visual tokenization during image synthesis, including continuous (Cont.) and discrete (Dist.) approaches. Entries by gray are expert models for T2I retrieval or generation, and those with a blue background denote that an image query is first generated and then used to perform image-to-image retrieval. Entries with a gray background denote our methods.

Method	Size	LLM	Token	CLIP-T \uparrow	CLIP-I \uparrow
<i>Text-to-Image Generation</i>					
SDXL [43]	2.6B	-	Cont.	26.79	46.71
GILL [24]	8B	OPT-6.7B	Cont.	14.16	13.72
Emu [55]	14B	LLaMA-13B	Cont.	22.26	40.78
Emu 2 [54]	37B	LLaMA-33B	Cont.	24.25	44.24
DreamLLM [7]	8B	Vicuna-7B	Cont.	24.34	42.77
SEED-LLaMA [14]	8B	LLaMA-7B	Dist.	22.00	43.02
LaVIT [20]	11B	LLaMA-7B	Dist.	27.07	48.75
<i>Text-to-Image Retrieval</i>					
CLIP (ViT-B/32) [46]	151M	-	Cont.	25.22	53.95
SDXL [43]	2.6B	-	Cont.	15.41	35.96
Emu [55]	14B	LLaMA-13B	Cont.	14.44	34.46
Emu 2 [54]	37B	LLaMA-33B	Cont.	14.69	36.38
DreamLLM [7]	8B	Vicuna-7B	Cont.	15.41	37.18
SEED-LLaMA [14]	8B	LLaMA-7B	Dist.	14.78	36.93
LaVIT [20]	11B	LLaMA-7B	Dist.	16.34	39.25
GILL [24]	8B	OPT-6.7B	Cont.	10.96	16.30
Ours (SEED-LLaMA)	8B	LLaMA-7B	Dist.	16.95	40.30
Ours (LaVIT)	11B	LLaMA-7B	Dist.	21.30	50.03
<i>Unified Text-to-Image Generation and Retrieval</i>					
GILL [24]	8B	OPT-6.7B	Cont.	12.12	15.25
Ours (SEED-LLaMA)	8B	LLaMA-7B	Dist.	23.98	50.52
Ours (LaVIT)	11B	LLaMA-7B	Dist.	28.45	61.37

above and choose the image with the higher similarity. Different from the retrieval process, which performs semantic matching within the database, this decision-making module may require stronger discriminative power from MLLMs due to the potential gap between generated and retrieved images.

4 TIGeR-Bench

To evaluate the performance of the unified problem, we build a comprehensive benchmark (TIGeR-Bench), as shown in Fig. 1. It covers creative and knowledge-intensive image acquisition domains.

Creative Domains. Human creative image requirements emphasize obtaining intricate visual content that is challenging to capture in the real world. This includes unusual and *counterfactual* compositions of concepts (*e.g.*, “A steamed train bellows rainbow-hued smoke”) and imaginary scenes that align with real users’ genuine creative *preference*. To meet the two aspects, we collect prompt-image pairs from the well-designed WHOOPS! [2] dataset and a large-scale open dataset named Pick-a-Pic [23] which stems from a web platform collecting real users’ creation intention, respectively.

Knowledge Domains. To acquire knowledge-intensive images, a model is required to have sufficient knowledge from specific vertical domains and disciplines. We focus on 6 knowledge domains including *logo* [60], *history and news* [38], *landmark* [63], *food* [41], *nature species* [59], *Wiki miscellaneous* [53], and collect text-image pairs from six high-quality datasets. Different from previous content-oriented image-text data [35, 68] including common things in daily life, the collected data focuses on the knowledge alignment across modalities, *e.g.*, the texts may only convey concept names without any descriptions in appearance.

Based on the two aspects of domains, we collect pairwise image-text data from 8 domains, constructing the evaluation benchmark containing 6,000 data samples, with 3,000 for creative domains and 3,000 for knowledge domains. See Appendix. A for more details of data sources, construction pipeline, and extension to long prompts and chat scenarios.

Table 3: Text-to-image retrieval performance comparison on Flickr30K and MS-COCO. Entries by gray denote dense retrieval methods and others are generative retrieval methods.

Method	Flickr30K (1K)			MS-COCO (5K)		
	R@1	R@5	R@10	R@1	R@5	R@10
CLIP (ViT-B/32) [46]	68.70	90.60	95.20	37.80	62.40	72.20
GRACE (Structured ID) [34]	37.40	59.50	66.20	16.70	39.20	50.30
IRGen [73]	49.00	68.90	72.50	29.60	50.70	56.30
Ours (LaVIT)	68.84	82.92	86.44	44.81	62.61	68.28
Ours (SEED-LLaMA)	71.70	91.82	95.44	46.11	69.02	76.13

Table 4: Ablation study on TIGeR-Bench investigating Reverse Re-Ranking (RRR) and two decision-making strategies, *i.e.*, Forward with Eqn. 3 and Reverse with Eqn. 4. %Retr. denotes the percentage of retrieved images selected as results.

RRR	Decision	Ours (SEED-LLaMA)				Ours (LaVIT)			
		CLIP-T \uparrow	CLIP-I \uparrow	R@1 \uparrow	%Retr.	CLIP-T \uparrow	CLIP-I \uparrow	R@1 \uparrow	%Retr.
	Forward	22.63	49.71	26.80	42.10	27.19	49.59	28.13	4.38
\checkmark	Forward	23.72	48.86	29.23	12.72	27.28	49.62	49.37	1.40
	Reverse	23.89	50.52	26.80	25.60	28.23	56.51	28.13	30.47
\checkmark	Reverse	22.84	49.54	29.23	61.47	28.45	61.37	49.37	56.25

5 Experiments

5.1 Datasets, Baselines, and Evaluation Metrics

We use the constructed TIGeR-Bench to evaluate the unified performance, and the two widely-used benchmark datasets, *i.e.*, Flickr30K [68] and MS-COCO [35], to assess the text-to-image retrieval performance. The compared baselines mainly include recent MLLMs [14, 20, 24, 54, 54, 55] which can generate images, as well as generation and retrieval expert models [43, 46]. Following T2I-G [9, 43, 51], the unified performance is measured by the CLIP score [17] including CLIP-T for text-image alignment and CLIP-I for the alignment between the predicted image and the ground-truth image. As for T2I-R [11, 17], we adopt the standard metric Recall at K, R@K (K=1, 5, and 10) for short. Details on datasets, baselines, and evaluation metrics are provided in Appendix. C.

5.2 Performance Comparison

Unified Performance on TIGeR-Bench. We compare MLLM baselines and our method and report the comprehensive results on TIGeR-Bench in Tab. 2, including separate and unified tasks. The results show that our proposed method achieves the best performance on the unified benchmark, compared with expert generation [43] or retrieval models [46], the state-of-the-art MLLMs, and GILL [24]. Due to half of the data being sourced from knowledge domains, current generation models, *e.g.*, SDXL [43], and MLLMs could not handle the unified problem well. Moreover, the proposed method could achieve impressive retrieval results, especially compared with other MLLMs or SDXL. Compared with the vanilla SEED-LLaMA and LaVIT, our method significantly improves the retrieval performance and enables them to deal with the unified problem.

Text-to-Image Retrieval Performance on Flickr30K [68] and MS-COCO [35]. As shown in Tab. 3, we compare the proposed method with the representative dense retrieval model CLIP [46] and two generative retrieval baselines [34, 73] which have been specially trained on the two datasets. In contrast, the proposed method is training-free but achieves the best performance across all baselines. It verifies the effectiveness of the proposed generative retrieval method and demonstrates that MLLMs are capable of retrieval despite the sole optimization objective of next-token prediction.

5.3 In-depth Analysis

Ablation Study on Reverse Re-Ranking (RRR) and Decision-Making for TIGeR. We evaluate the proposed method based on SEED-LLaMA and LaVIT on TIGeR by different RRR and decision settings, and report the unified and retrieval performance as well as the retrieval percentage in Tab. 4. Based on the results, we have the following discussions: 1) RRR could consistently improve the retrieval performance for SEED-LLaMA and LaVIT, but may not help in unified performance for

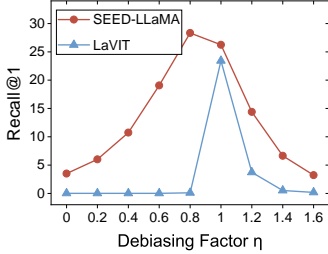


Figure 3: The influence of the debiasing factor η in Eqn. 3 on the forward ranking performance of SEED-LLaMA and LaVIT on the MS-COCO dataset. The best performance is achieved around $\eta = 1$.

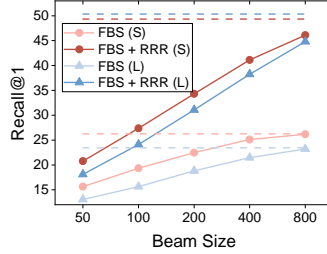


Figure 4: Retrieval performance on MS-COCO with different beam sizes and re-ranking strategies. Light and dark dash lines denote the forward and reverse ranking performance, respectively. S: SEED-LLaMA. L: LaVIT.

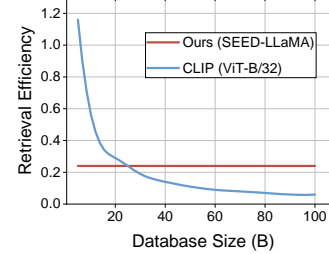


Figure 5: Comparison of retrieval efficiency quantified by the number of processed queries per second between CLIP-B and the proposed generative retrieval based on SEED-LLaMA.

SEED-LLaMA, because unified performance is also influenced by decision strategies. 2) Compared with the forward decision with Eqn. 3, the reverse decision with Eqn 4 could enhance the unified performance in most cases for both models, which reflects the reverse decision may have stronger discriminative power across more domains. 3) Intuitively, we expect the most correctly retrieved images can be selected and the left wrong ones can be remedied by generation. However, we find that the two MLLMs may suffer from a generation preference problem. Especially, LaVIT always prefers to choose generated images even though the retrieved images are correct, as shown by the low %Retr. in the first two settings. One of the reasons may be that there is significant gaps between the pre-trained and fine-tuned image generation data and the TIGer-Bench. In all, in addition to the modality bias discussed in Tab. 1, the difference between the two directional ranking and decision may be attributed to the unbalance between captioning (image-to-text) and text-to-image data during the training phase of MLLMs.

Visual Modality Debiasing for Discriminative Power. In Sec. 3.3, we discussed the visual modality bias problem with the forward $\log p(Y|X)$ in Eqn. 2 as the similarity proxy, and adopt a debiasing strategy $\log \frac{p(Y|X)}{p(Y)}$ by considering the unconditional likelihood. To explore the influence of the debiasing strength, we set different values of the factor η in Eqn. 3 and a series of results are shown in Fig. 3. They show that the ranking performance is sensitive to the debiasing strength and reaches the highest point around $\eta = 1$, verifying the effectiveness of the unconditional debiasing strategy.

Forward Beam Search (FBS) and Reverse Re-Ranking for Retrieval. Considering the trade-off of retrieval efficiency and recall, we present FBS and RRR, respectively. As shown in Fig. 4, we compare the ranking (dotted lines) and retrieval performance (solid lines) and explore the impact of beam size and RRR. In the ranking experiments, we adopt the proxies in Sec. 3.3 to calculate similarities, and then rank the whole database based on which. The comparison results demonstrate that ranking with the forward $\log \frac{p(Y|X)}{p(Y)}$ seems the upper bound of FBS since FBS may miss the target image with the limited beam size. Benefiting from the reverse matching proxy $\log p(X|Y)$, RRR could help FBS break through the ceiling and significantly improve recall. Additionally, regardless of similarity proxies or base MLLMs employed, increasing the beam size can reduce the recall gap between retrieval and ranking.

Efficiency of Generative Retrieval. We analyze the efficiency of the proposed generative retrieval method for T2I-R and compare it with that of the representative dense retrieval method CLIP [46] in Fig. 5. The efficiency of dense retrieval gets worse with the increase in the database size due to more matching in the common feature space. In contrast, the proposed method keeps constant efficiency regardless of the database size. We relegate more efficiency analysis to Appendix. C.2.

5.4 Qualitative Analysis

In Fig. 6, we compare our methods with SDXL on TIGer-Bench, covering both creative and knowledge domains. SDXL, despite its strong generative abilities, struggles in knowledge domains. In contrast, our method excavates the intrinsic discriminative power of MLLMs and endows them



Figure 6: Qualitative results on TIGeR-Bench. The prefix prompt "Give me an image of" is omitted here. Green ticks and red crosses highlight correct and wrong retrieval results.

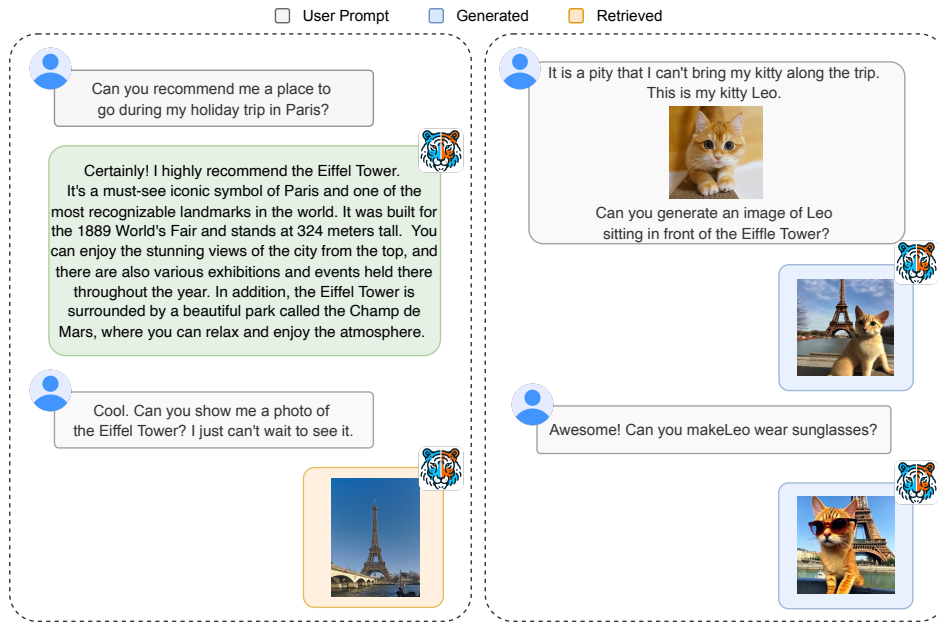


Figure 7: Example of multi-turn chat based on SEED-LLaMA with unified generation and retrieval.

with the retrieval ability, enabling more effective handling for knowledge-intensive image acquisition. Besides, we explore more complicated multi-turn chat scenarios with multimodal context and both image retrieval and generation or editing requirements in Fig. 7. Seamlessly integrated into MLLMs without training and benefiting from multimodal instruction tuning, the proposed model inherits the basic multimodal understanding, generation, and user intention capturing capabilities of MLLMs and meanwhile shows potential for knowledge-intensive tasks in vertical domains.

6 Conclusion

In this work, we start with the practical requirements for image acquisition, analyze the weaknesses of single generation and retrieval, and propose to unify these two tasks within MLLMs. Toward this end, we first delve into the intrinsic discriminative abilities of MLLMs for semantic matching and propose a generative retrieval method to perform text-to-image retrieval in an auto-regressive manner. Besides, under the same auto-regressive framework, we unify generation and retrieval synchronously and present an autonomous decision strategy to select the best image. The proposed framework exhibited effectiveness and versatility across the constructed TIGeR-Bench and two retrieval benchmarks.

References

- [1] James Betker, Gabriel Goh, Li Jing, Tim Brooks, Jianfeng Wang, Linjie Li, Long Ouyang, Juntang Zhuang, Joyce Lee, Yufei Guo, et al. Improving image generation with better captions. *Computer Science*. <https://cdn.openai.com/papers/dall-e-3.pdf>, 2(3):8, 2023.
- [2] Nitzan Bitton-Guetta, Yonatan Bitton, Jack Hessel, Ludwig Schmidt, Yuval Elovici, Gabriel Stanovsky, and Roy Schwartz. Breaking common sense: Whoops! a vision-and-language benchmark of synthetic and compositional images. In *Proceedings of the IEEE/CVF International Conference on Computer Vision*, pages 2616–2627, 2023.
- [3] Hila Chefer, Yuval Alaluf, Yael Vinker, Lior Wolf, and Daniel Cohen-Or. Attend-and-excite: Attention-based semantic guidance for text-to-image diffusion models. *ACM Transactions on Graphics (TOG)*, 42(4):1–10, 2023.
- [4] Kevin Clark and Priyank Jaini. Text-to-image diffusion models are zero-shot classifiers. *arXiv preprint arXiv:2303.15233*, 2023.
- [5] Prafulla Dhariwal and Alexander Nichol. Diffusion models beat gans on image synthesis. *Advances in neural information processing systems*, 34:8780–8794, 2021.
- [6] Ming Ding, Zhuoyi Yang, Wenyi Hong, Wendi Zheng, Chang Zhou, Da Yin, Junyang Lin, Xu Zou, Zhou Shao, Hongxia Yang, et al. Cogview: Mastering text-to-image generation via transformers. *Advances in Neural Information Processing Systems*, 34:19822–19835, 2021.
- [7] Runpei Dong, Chunrui Han, Yuang Peng, Zekun Qi, Zheng Ge, Jinrong Yang, Liang Zhao, Jianjian Sun, Hongyu Zhou, Haoran Wei, et al. Dreamllm: Synergistic multimodal comprehension and creation. *arXiv preprint arXiv:2309.11499*, 2023.
- [8] Zi-Yi Dou, Yichong Xu, Zhe Gan, Jianfeng Wang, Shuohang Wang, Lijuan Wang, Chenguang Zhu, Pengchuan Zhang, Lu Yuan, Nanyun Peng, et al. An empirical study of training end-to-end vision-and-language transformers. In *Proceedings of the IEEE/CVF Conference on Computer Vision and Pattern Recognition*, pages 18166–18176, 2022.
- [9] Patrick Esser, Sumith Kulal, Andreas Blattmann, Rahim Entezari, Jonas Müller, Harry Saini, Yam Levi, Dominik Lorenz, Axel Sauer, Frederic Boesel, et al. Scaling rectified flow transformers for high-resolution image synthesis. *arXiv preprint arXiv:2403.03206*, 2024.
- [10] Patrick Esser, Robin Rombach, and Bjorn Ommer. Taming transformers for high-resolution image synthesis. In *Proceedings of the IEEE/CVF conference on computer vision and pattern recognition*, pages 12873–12883, 2021.
- [11] Fartash Faghri, David J Fleet, Jamie Ryan Kiros, and Sanja Fidler. Vse++: Improving visual-semantic embeddings with hard negatives. *arXiv preprint arXiv:1707.05612*, 2017.
- [12] Weixi Feng, Xuehai He, Tsu-Jui Fu, Varun Jampani, Arjun Akula, Pradyumna Narayana, Sugato Basu, Xin Eric Wang, and William Yang Wang. Training-free structured diffusion guidance for compositional text-to-image synthesis. *arXiv preprint arXiv:2212.05032*, 2022.
- [13] Markus Freitag and Yaser Al-Onaizan. Beam search strategies for neural machine translation. *arXiv preprint arXiv:1702.01806*, 2017.
- [14] Yuying Ge, Sijie Zhao, Ziyun Zeng, Yixiao Ge, Chen Li, Xintao Wang, and Ying Shan. Making llama see and draw with seed tokenizer. *arXiv preprint arXiv:2310.01218*, 2023.
- [15] Will Grathwohl, Kuan-Chieh Wang, Jörn-Henrik Jacobsen, David Duvenaud, Mohammad Norouzi, and Kevin Swersky. Your classifier is secretly an energy based model and you should treat it like one. *arXiv preprint arXiv:1912.03263*, 2019.
- [16] Xuehai He, Weixi Feng, Tsu-Jui Fu, Varun Jampani, Arjun Akula, Pradyumna Narayana, Sugato Basu, William Yang Wang, and Xin Eric Wang. Discriminative diffusion models as few-shot vision and language learners. *arXiv preprint arXiv:2305.10722*, 2023.
- [17] Jack Hessel, Ari Holtzman, Maxwell Forbes, Ronan Le Bras, and Yejin Choi. Clipscore: A reference-free evaluation metric for image captioning. *arXiv preprint arXiv:2104.08718*, 2021.

- [18] Jonathan Ho, Ajay Jain, and Pieter Abbeel. Denoising diffusion probabilistic models. *Advances in neural information processing systems*, 33:6840–6851, 2020.
- [19] Wen Huang, Hongbin Liu, Minxin Guo, and Neil Zhenqiang Gong. Visual hallucinations of multi-modal large language models. *arXiv preprint arXiv:2402.14683*, 2024.
- [20] Yang Jin, Kun Xu, Kun Xu, Liwei Chen, Chao Liao, Jianchao Tan, Quzhe Huang, Bin Chen, Chenyi Lei, An Liu, et al. Unified language-vision pretraining in llm with dynamic discrete visual tokenization. *arXiv e-prints*, pages arXiv–2309, 2023.
- [21] Jared Kaplan, Sam McCandlish, Tom Henighan, Tom B Brown, Benjamin Chess, Rewon Child, Scott Gray, Alec Radford, Jeffrey Wu, and Dario Amodei. Scaling laws for neural language models. *arXiv preprint arXiv:2001.08361*, 2020.
- [22] Seunghoi Kim, Chen Jin, Tom Diethe, Matteo Figini, Henry FJ Tregidgo, Asher Mullokandov, Philip Teare, and Daniel C Alexander. Tackling structural hallucination in image translation with local diffusion. *arXiv preprint arXiv:2404.05980*, 2024.
- [23] Yuval Kirstain, Adam Polyak, Uriel Singer, Shahbuland Matiana, Joe Penna, and Omer Levy. Pick-a-pic: An open dataset of user preferences for text-to-image generation. *Advances in Neural Information Processing Systems*, 36, 2024.
- [24] Jing Yu Koh, Daniel Fried, and Ruslan Salakhutdinov. Generating images with multimodal language models. *arXiv preprint arXiv:2305.17216*, 2023.
- [25] Benno Krojer, Elinor Poole-Dayana, Vikram Voleti, Christopher Pal, and Siva Reddy. Are diffusion models vision-and-language reasoners? In *Thirty-seventh Conference on Neural Information Processing Systems*, 2023.
- [26] Kimin Lee, Hao Liu, Moonkyung Ryu, Olivia Watkins, Yuqing Du, Craig Boutilier, Pieter Abbeel, Mohammad Ghavamzadeh, and Shixiang Shane Gu. Aligning text-to-image models using human feedback. *arXiv preprint arXiv:2302.12192*, 2023.
- [27] Kuang-Huei Lee, Xi Chen, Gang Hua, Houdong Hu, and Xiaodong He. Stacked cross attention for image-text matching. In *Proceedings of the European conference on computer vision (ECCV)*, pages 201–216, 2018.
- [28] Matan Levy, Rami Ben-Ari, Nir Darshan, and Dani Lischinski. Chatting makes perfect: Chat-based image retrieval. *Advances in Neural Information Processing Systems*, 36, 2024.
- [29] Alexander C Li, Mihir Prabhudesai, Shivam Duggal, Ellis Brown, and Deepak Pathak. Your diffusion model is secretly a zero-shot classifier. *arXiv preprint arXiv:2303.16203*, 2023.
- [30] Hao Li, Yang Zou, Ying Wang, Orchid Majumder, Yusheng Xie, R Manmatha, Ashwin Swaminathan, Zhuowen Tu, Stefano Ermon, and Stefano Soatto. On the scalability of diffusion-based text-to-image generation. *arXiv preprint arXiv:2404.02883*, 2024.
- [31] Junnan Li, Dongxu Li, Silvio Savarese, and Steven Hoi. Blip-2: Bootstrapping language-image pre-training with frozen image encoders and large language models. *arXiv preprint arXiv:2301.12597*, 2023.
- [32] Junnan Li, Ramprasaath Selvaraju, Akhilesh Gotmare, Shafiq Joty, Caiming Xiong, and Steven Chu Hong Hoi. Align before fuse: Vision and language representation learning with momentum distillation. *Advances in neural information processing systems*, 34:9694–9705, 2021.
- [33] Kunpeng Li, Yulun Zhang, Kai Li, Yuanyuan Li, and Yun Fu. Visual semantic reasoning for image-text matching. In *Proceedings of the IEEE/CVF international conference on computer vision*, pages 4654–4662, 2019.
- [34] Yongqi Li, Wenjie Wang, Leigang Qu, Liqiang Nie, Wenjie Li, and Tat-Seng Chua. Generative cross-modal retrieval: Memorizing images in multimodal language models for retrieval and beyond. *arXiv preprint arXiv:2402.10805*, 2024.

- [35] Tsung-Yi Lin, Michael Maire, Serge Belongie, James Hays, Pietro Perona, Deva Ramanan, Piotr Dollár, and C Lawrence Zitnick. Microsoft coco: Common objects in context. In *Computer Vision—ECCV 2014: 13th European Conference, Zurich, Switzerland, September 6-12, 2014, Proceedings, Part V 13*, pages 740–755. Springer, 2014.
- [36] Weizhe Lin, Jingbiao Mei, Jinghong Chen, and Bill Byrne. Preflmr: Scaling up fine-grained late-interaction multi-modal retrievers. *arXiv preprint arXiv:2402.08327*, 2024.
- [37] Zhiqiu Lin, Xinyue Chen, Deepak Pathak, Pengchuan Zhang, and Deva Ramanan. Revisiting the role of language priors in vision-language models. 2024.
- [38] Fuxiao Liu, Yinghan Wang, Tianlu Wang, and Vicente Ordonez. Visual news: Benchmark and challenges in news image captioning. *arXiv preprint arXiv:2010.03743*, 2020.
- [39] Haotian Liu, Chunyuan Li, Qingyang Wu, and Yong Jae Lee. Visual instruction tuning. *arXiv preprint arXiv:2304.08485*, 2023.
- [40] Jiasen Lu, Christopher Clark, Sangho Lee, Zichen Zhang, Savya Khosla, Ryan Marten, Derek Hoiem, and Aniruddha Kembhavi. Unified-io 2: Scaling autoregressive multimodal models with vision, language, audio, and action. *arXiv preprint arXiv:2312.17172*, 2023.
- [41] Weiqing Min, Zhiling Wang, Yuxin Liu, Mengjiang Luo, Liping Kang, Xiaoming Wei, Xiaolin Wei, and Shuqiang Jiang. Large scale visual food recognition. *IEEE Transactions on Pattern Analysis and Machine Intelligence*, 2023.
- [42] Long Ouyang, Jeffrey Wu, Xu Jiang, Diogo Almeida, Carroll Wainwright, Pamela Mishkin, Chong Zhang, Sandhini Agarwal, Katarina Slama, Alex Ray, et al. Training language models to follow instructions with human feedback. *Advances in neural information processing systems*, 35:27730–27744, 2022.
- [43] Dustin Podell, Zion English, Kyle Lacey, Andreas Blattmann, Tim Dockhorn, Jonas Müller, Joe Penna, and Robin Rombach. Sdxl: Improving latent diffusion models for high-resolution image synthesis. *arXiv preprint arXiv:2307.01952*, 2023.
- [44] Leigang Qu, Meng Liu, Jianlong Wu, Zan Gao, and Liqiang Nie. Dynamic modality interaction modeling for image-text retrieval. In *Proceedings of the 44th International ACM SIGIR Conference on Research and Development in Information Retrieval*, pages 1104–1113, 2021.
- [45] Leigang Qu, Wenjie Wang, Yongqi Li, Hanwang Zhang, Liqiang Nie, and Tat-Seng Chua. Discriminative probing and tuning for text-to-image generation. *arXiv preprint arXiv:2403.04321*, 2024.
- [46] Alec Radford, Jong Wook Kim, Chris Hallacy, Aditya Ramesh, Gabriel Goh, Sandhini Agarwal, Girish Sastry, Amanda Askell, Pamela Mishkin, Jack Clark, et al. Learning transferable visual models from natural language supervision. In *International conference on machine learning*, pages 8748–8763. PMLR, 2021.
- [47] Aditya Ramesh, Prafulla Dhariwal, Alex Nichol, Casey Chu, and Mark Chen. Hierarchical text-conditional image generation with clip latents. *arXiv preprint arXiv:2204.06125*, 1(2):3, 2022.
- [48] Aditya Ramesh, Mikhail Pavlov, Gabriel Goh, Scott Gray, Chelsea Voss, Alec Radford, Mark Chen, and Ilya Sutskever. Zero-shot text-to-image generation. In *International Conference on Machine Learning*, pages 8821–8831. PMLR, 2021.
- [49] Scott Reed, Zeynep Akata, Xinchun Yan, Lajanugen Logeswaran, Bernt Schiele, and Honglak Lee. Generative adversarial text to image synthesis. In *International conference on machine learning*, pages 1060–1069. PMLR, 2016.
- [50] Robin Rombach, Andreas Blattmann, Dominik Lorenz, Patrick Esser, and Björn Ommer. High-resolution image synthesis with latent diffusion models. In *Proceedings of the IEEE/CVF conference on computer vision and pattern recognition*, pages 10684–10695, 2022.

- [51] Chitwan Saharia, William Chan, Saurabh Saxena, Lala Li, Jay Whang, Emily L Denton, Kamyar Ghasemipour, Raphael Gontijo Lopes, Burcu Karagol Ayan, Tim Salimans, et al. Photorealistic text-to-image diffusion models with deep language understanding. *Advances in Neural Information Processing Systems*, 35:36479–36494, 2022.
- [52] Christoph Schuhmann, Romain Beaumont, Richard Vencu, Cade Gordon, Ross Wightman, Mehdi Cherti, Theo Coombes, Aarush Katta, Clayton Mullis, Mitchell Wortsman, et al. Laion-5b: An open large-scale dataset for training next generation image-text models. *Advances in Neural Information Processing Systems*, 35:25278–25294, 2022.
- [53] Krishna Srinivasan, Karthik Raman, Jiecao Chen, Michael Bendersky, and Marc Najork. Wit: Wikipedia-based image text dataset for multimodal multilingual machine learning. In *Proceedings of the 44th International ACM SIGIR Conference on Research and Development in Information Retrieval*, pages 2443–2449, 2021.
- [54] Quan Sun, Yufeng Cui, Xiaosong Zhang, Fan Zhang, Qiyong Yu, Zhengxiong Luo, Yueze Wang, Yongming Rao, Jingjing Liu, Tiejun Huang, et al. Generative multimodal models are in-context learners. *arXiv preprint arXiv:2312.13286*, 2023.
- [55] Quan Sun, Qiyong Yu, Yufeng Cui, Fan Zhang, Xiaosong Zhang, Yueze Wang, Hongcheng Gao, Jingjing Liu, Tiejun Huang, and Xinlong Wang. Generative pretraining in multimodality. *arXiv preprint arXiv:2307.05222*, 2023.
- [56] Yi Tay, Vinh Tran, Mostafa Dehghani, Jianmo Ni, Dara Bahri, Harsh Mehta, Zhen Qin, Kai Hui, Zhe Zhao, Jai Gupta, et al. Transformer memory as a differentiable search index. *Advances in Neural Information Processing Systems*, 35:21831–21843, 2022.
- [57] Hugo Touvron, Louis Martin, Kevin Stone, Peter Albert, Amjad Almahairi, Yasmine Babaei, Nikolay Bashlykov, Soumya Batra, Prajjwal Bhargava, Shruti Bhosale, et al. Llama 2: Open foundation and fine-tuned chat models. *arXiv preprint arXiv:2307.09288*, 2023.
- [58] Aaron Van Den Oord, Oriol Vinyals, et al. Neural discrete representation learning. *Advances in neural information processing systems*, 30, 2017.
- [59] Grant Van Horn, Oisín Mac Aodha, Yang Song, Yin Cui, Chen Sun, Alex Shepard, Hartwig Adam, Pietro Perona, and Serge Belongie. The inaturalist species classification and detection dataset. In *Proceedings of the IEEE conference on computer vision and pattern recognition*, pages 8769–8778, 2018.
- [60] Jing Wang, Weiqing Min, Sujuan Hou, Shengnan Ma, Yuanjie Zheng, Haishuai Wang, and Shuqiang Jiang. Logo-2k+: A large-scale logo dataset for scalable logo classification. In *Proceedings of the AAAI Conference on Artificial Intelligence*, volume 34, pages 6194–6201, 2020.
- [61] Tan Wang, Kevin Lin, Linjie Li, Chung-Ching Lin, Zhengyuan Yang, Hanwang Zhang, Zicheng Liu, and Lijuan Wang. Equivariant similarity for vision-language foundation models. In *Proceedings of the IEEE/CVF International Conference on Computer Vision*, pages 11998–12008, 2023.
- [62] Cong Wei, Yang Chen, Haonan Chen, Hexiang Hu, Ge Zhang, Jie Fu, Alan Ritter, and Wenhui Chen. Uniir: Training and benchmarking universal multimodal information retrievers. *arXiv preprint arXiv:2311.17136*, 2023.
- [63] Tobias Weyand, Andre Araujo, Bingyi Cao, and Jack Sim. Google landmarks dataset v2-a large-scale benchmark for instance-level recognition and retrieval. In *Proceedings of the IEEE/CVF conference on computer vision and pattern recognition*, pages 2575–2584, 2020.
- [64] Shengqiong Wu, Hao Fei, Leigang Qu, Wei Ji, and Tat-Seng Chua. Next-gpt: Any-to-any multimodal llm. *arXiv preprint arXiv:2309.05519*, 2023.
- [65] Xiaoshi Wu, Keqiang Sun, Feng Zhu, Rui Zhao, and Hongsheng Li. Better aligning text-to-image models with human preference. *arXiv preprint arXiv:2303.14420*, 2023.

- [66] Jiazheng Xu, Xiao Liu, Yuchen Wu, Yuxuan Tong, Qinkai Li, Ming Ding, Jie Tang, and Yuxiao Dong. Imagereward: Learning and evaluating human preferences for text-to-image generation. *Advances in Neural Information Processing Systems*, 36, 2024.
- [67] Ling Yang, Zhaochen Yu, Chenlin Meng, Minkai Xu, Stefano Ermon, and Bin Cui. Mastering text-to-image diffusion: Recaptioning, planning, and generating with multimodal llms. *arXiv preprint arXiv:2401.11708*, 2024.
- [68] Peter Young, Alice Lai, Micah Hodosh, and Julia Hockenmaier. From image descriptions to visual denotations: New similarity metrics for semantic inference over event descriptions. *Transactions of the Association for Computational Linguistics*, 2:67–78, 2014.
- [69] Jiahui Yu, Zirui Wang, Vijay Vasudevan, Legg Yeung, Mojtaba Seyedhosseini, and Yonghui Wu. Coca: Contrastive captioners are image-text foundation models. *arXiv preprint arXiv:2205.01917*, 2022.
- [70] Jiahui Yu, Yuanzhong Xu, Jing Yu Koh, Thang Luong, Gunjan Baid, Zirui Wang, Vijay Vasudevan, Alexander Ku, Yinfei Yang, Burcu Karagol Ayan, et al. Scaling autoregressive models for content-rich text-to-image generation. *arXiv preprint arXiv:2206.10789*, 2022.
- [71] Lili Yu, Bowen Shi, Ramakanth Pasunuru, Benjamin Muller, Olga Golovneva, Tianlu Wang, Arun Babu, Binh Tang, Brian Karrer, Shelly Sheynin, et al. Scaling autoregressive multi-modal models: Pretraining and instruction tuning. *arXiv preprint arXiv:2309.02591*, 2(3), 2023.
- [72] Jiaqi Zhai, Lucy Liao, Xing Liu, Yueming Wang, Rui Li, Xuan Cao, Leon Gao, Zhaojie Gong, Fangda Gu, Michael He, et al. Actions speak louder than words: Trillion-parameter sequential transducers for generative recommendations. *arXiv preprint arXiv:2402.17152*, 2024.
- [73] Yidan Zhang, Ting Zhang, Dong Chen, Yujing Wang, Qi Chen, Xing Xie, Hao Sun, Weiwei Deng, Qi Zhang, Fan Yang, et al. Irgen: Generative modeling for image retrieval. *arXiv preprint arXiv:2303.10126*, 2023.
- [74] Kaizhi Zheng, Xuehai He, and Xin Eric Wang. Minigpt-5: Interleaved vision-and-language generation via generative vokens. *arXiv preprint arXiv:2310.02239*, 2023.
- [75] Deyao Zhu, Jun Chen, Xiaoqian Shen, Xiang Li, and Mohamed Elhoseiny. Minigpt-4: Enhancing vision-language understanding with advanced large language models. *arXiv preprint arXiv:2304.10592*, 2023.
- [76] Jinguo Zhu, Xiaohan Ding, Yixiao Ge, Yuying Ge, Sijie Zhao, Hengshuang Zhao, Xiaohua Wang, and Ying Shan. Vl-gpt: A generative pre-trained transformer for vision and language understanding and generation. *arXiv preprint arXiv:2312.09251*, 2023.

A TIGeR-Bench Details

A.1 Data Collection

Data Source. To comprehensively evaluate unified text-to-image generation and retrieval, we build a benchmark called TIGeR-Bench, encompassing both creative and knowledge-intensive domains. For the creative domains, the data is derived from authentic user prompts that reflect real-world needs, requiring high levels of novelty and creativity. We collect the data from the WHOOPS! [2] and Pick-a-Pic [23] datasets:

- **WHOOPS!** [2]: The WHOOPS! dataset consists of 500 commonsense-defying prompt-image pairs created by designers. First, the designers think of counterfactual prompts by combining two elements or concepts that violate commonsense, *e.g.*, “Albert Einstein holding a smartphone”. Next, they are guided to use text-to-image generation tools (*e.g.*, Midjourney, DALL-E [48], and Stable Diffusion [50]) to synthesize images using these counterfactual prompts. Finally, the designers verify the ‘weirdness’ of generated images to guarantee the data quality.
- **Pick-a-Pic** [2]: The Pick-a-Pic dataset consists of real-world user prompts and corresponding generated images, annotated with user preference, gathered from the Pick-a-Pic web application. In detail, we collect our data from Pick-a-Pic v2 ³.

For knowledge-intensive domains, we collect data encompassing a wide range of categories to fulfill users’ needs for visual knowledge, including Logo-2K+ [60], Visual News [38], Google Landmark v2 [63], Food2k [41], iNaturalist [59], WIT [23].

- **Logo-2K+** [60]: Logo-2K+ is a large-scale real-world logo dataset, containing 167,140 images with 2,341 categories and 10 root categories, *e.g.*, food, clothes, and institution.
- **Visual News** [38]: Visual News is a large-scale dataset comprising over one million news images along with associated news articles, image captions, author information, and additional metadata. Distinguished from other image captioning datasets, this dataset prioritizes factual contexts, including individuals, locations, and events, sourced from prominent news outlets such as The Guardian, BBC, USA Today, and The Washington Post.
- **Google Landmark v2** [38]: Google Landmark v2 includes approximately 5M images annotated with 200k distinct instance labels representing human-made and natural landmarks. It is collected from Wikimedia Commons.
- **Food2K** [41]: Food2K is a food recognition dataset with 2,000 categories and more than 1 million images, covering cereal products, vegetables, bread, snack, soup and porridge, barbecue, egg products, dessert, bean products, seafood, fried food, and meat.
- **iNaturalist** [59]: The iNaturalist dataset is constructed to reflect the diversity of the natural world, featuring an unbalanced distribution of species. It encompasses a total of 5,000 species of plants and animals, accompanied by 859,000 images.
- **WIT** [23]: Wikipedia-based Image Text (WIT) is a large multimodal multilingual dataset, comprising 37.6 million image-text pairs representing real-world entities. It encompasses 11.5 million unique images across 108 Wikipedia languages. The texts are sourced from 3 primary channels: reference descriptions, attribution descriptions, and alt-text descriptions.

Prompts. The WHOOPS! and Pick-a-Pic datasets contain prompts, while Visual News also provides natural language descriptions, serving as user prompts or queries. For the remaining five datasets, only category names or concepts represented by single words or phrases are available. To address this, we utilize a template to formulate them into complete prompt sentences, *i.e.*, “Give me an image of [concept]”.

These datasets, originally designed for different purposes, are effectively repurposed as the creative domain and knowledge-intensive domain candidates within the TIGeR-Bench.

³https://huggingface.co/datasets/yuvalkirstain/pickapic_v2

Table 5: The statistics of TIGeR-Bench. We keep the ratio of 1 : 1 for creative and knowledge domains and collect 6,000 high-quality text-image pairs in total.

Domain	Data Source	#Text-Image Pairs
Creative	WHOOPS! [2]	500
	Pick-a-Pic [23]	2500
Knowledge-intensive	Logo-2K+ [60]	500
	Visual News [38]	500
	Google Landmark v2 [63]	500
	Food2K [41]	500
	iNaturalist [59]	500
	WIT [23]	500

A.2 Automatic Data Filtration

Data Split. To evaluate text-to-image generation and retrieval, we prioritize selecting the original test split of each dataset to construct TIGeR-Bench. In cases where only a validation set is provided, we default to utilizing the validation set.

Filtration Pipeline Given that all 8 datasets have undergone individual single-modality quality assessments during their construction, our emphasis now lies on cross-modal relevance and generation challenge properties. We proceed with the following three steps for data filtration.

- 1) To ensure a strong alignment between the positive text and image pairs for both generation and retrieval, we employ a filtering process to remove weakly relevant text-image pairs (*e.g.*, outliers or noisy pairs) across 7 datasets except for WHOOPS! due to its limited scale. Specifically, we calculate the CLIP-T scores (S_{gt}) between the ground-truth images and texts, and remove pairs with CLIP-T scores lower than 30.0. Considering the large scale of Pick-a-Pic, we then randomly sample 7,500 pairs as candidates for the following human quality validation phase.
- 2) As discussed in Sec. 1, T2I-G models may struggle with synthesizing knowledge-intensive images. To identify challenging concepts in the above six knowledge-intensive datasets, which pose difficulties for current state-of-the-art T2I-G models, we first employ open-sourced models including the SD series [43, 50] to generate images by feeding the textual prompts in candidates as conditional input. Subsequently, we calculate the average CLIP-T scores (S_{gen}) over images generated by multiple models for each prompt. We then calculate the difference between the scores of the ground-truth pair and the generated pair for each prompt, *i.e.*, $\Delta = S_{gt} - S_{gen}$.
- 3) Finally, we select the top 1,000 unique instance pairs – comprising 1,000 different prompts and 1,000 different images – with the highest values of Δ for each knowledge dataset. The remaining examples form a new candidate set with 500 WHOOPS! instances, 7,500 Pick-a-Pic instances, and 1,000 instances for the six knowledge datasets.

A.3 Human Annotator Filtration

To further improve the data quality of TIGeR-Bench, human annotators were employed to mark evaluate each text-image pair across three aspects: text, image, and pair. Specifically, as for each text-image pair, considerations include the conciseness and unambiguity of the text, the clarity and usefulness of the image, and the relevance of the text-image pair. Annotators assigned a score of 0 (not satisfied) or 1 (satisfied) for each aspect. Finally, only text-image pairs meeting satisfaction across all three aspects were retained.

A.4 Data Sampling

To strike a balance between adequacy and efficiency in evaluation, we retain all 500 samples in WHOOPS!, and further randomly sample 2,500 data instances from Pick-a-Pic, along with 500 instances from each knowledge-intensive dataset. The statistics of TIGeR-Bench are presented in

Fig. 5. Maintaining a balanced ratio of 1 : 1 between creative and knowledge domains, we finally obtain a total of 6,000 high-quality text-image pairs.

B Model Details

In this work, we introduce and implement our approach for unified text-to-image generation and retrieval, based on two foundation MLLMs: SEED-LLaMA [14] and LaVIT [20]. The details of these two models are as follows.

SEED-LLaMA produces 32 discrete visual codes for each image via the SEED tokenizer. This tokenizer is composed of a Causal Q-Former, a learnable codebook, and an MLP (only for training), and is trained with contrastive learning and reconstruction objectives. SEED-LLaMA takes discrete visual codes as input for multimodal understanding tasks such as image captioning and VQA, and outputs discrete visual codes. The output codes are then fed into the unCLIP-SD model [47, 50] to generate images.

LaVIT obtains discrete visual codes with variable lengths using a meticulously designed dynamic visual tokenizer, which comprises a token selector, a token merger, and a reconstruction decoder (used solely for training). This tokenizer is trained with a reconstruction objective. During tokenization, LaVIT samples a binary decision mask from a Gumbel distribution to select visual patches and quantize them into discrete tokens. To ensure reproducibility and stability in tokenization, we depart from LaVIT and employ a deterministic selection method, where a patch is selected if its importance score exceeds a threshold of 0.5; otherwise, it is discarded. With this discriminative tokenization strategy, we pre-tokenize the 6 knowledge-intensive datasets of TIGeR-Bench, resulting in average, maximum, and minimum lengths of discrete tokens at 88, 130, and 37, respectively. During image generation, LaVIT first autoregressively produces a sequence of discrete visual tokens and then decodes them into an image using a diffusion model initialized with SD-v1.5 [50] or SDXL [43]. In contrast to SEED-LLaMA, which utilizes discrete visual tokens as input for multimodal understanding and generation, LaVIT takes continuous visual features from the token merger as input.

C Experimental Details

C.1 Baselines

As shown in Tab. 2, we compare the proposed method with several baselines on TIGeR-Bench across three aspects, *i.e.*, text-to-image generation, text-to-image retrieval, and unified generation and retrieval. We introduce these baselines in the following.

- **Text-to-Image Generation Baselines:** These include the expert model SDXL [43] and recent MLLMs with image generation abilities. The MLLMs in this category are GILL [24], Emu [55], Emu 2 [54], DreamLLM [7], SEED-LLaMA [14], and LaVIT [20].
- **Text-to-Image Retrieval Baselines:** These include the expert model CLIP (ViT-B/32) [46] and recent MLLMs. Currently, GILL [24] is the only MLLM with retrieval ability, which maps the embeddings of special visual tokens into the CLIP feature space. Although other MLLMs [7, 14, 20, 54, 55] do not directly support text-to-image retrieval, we evaluate them through a two-step process: 1) generating an image query conditioned on the text prompt, and 2) performing nearest neighbor search for image-to-image retrieval using the CLIP (ViT-B/32) image encoder as the feature extractor and cosine similarity as the metric.
- **Unified Text-to-Image Generation and Retrieval:** GILL [24] is the only baseline capable of performing both text-to-image generation and retrieval. It incorporates and trains a binary classifier to decide between generation and retrieval tasks.

C.2 Implementation Details

The proposed method is training-free and based on SEED-LLaMA [14] and LaVIT [20]. We utilize the 8B version of SEED-LLaMA and load the parameters of supervised fine-tuning. For LaVIT, we employ the 11B model with SDXL as the pixel decoder. We combine all images in the 6 knowledge-intensive datasets and tokenize them into discrete tokens. Subsequently, we build the mapping

Table 6: Unified performance comparison on the *CLIP-T score* across 8 domains in TIGeR-Bench.

Method	Creative Domains		Logo	News	Knowledge Domains		Food	Wiki	All
	Counterfactual	Preference			Landmark	Nature			
SDXL [43]	36.90	30.09	16.36	24.96	21.51	26.00	24.25	20.99	26.79
CLIP (ViT-B/32) [46]	16.61	15.86	36.17	34.95	32.51	30.56	29.44	31.00	24.21
GILL [24]	10.80	11.22	14.65	9.49	14.31	12.92	13.64	13.55	12.12
Emu [55]	23.61	23.98	17.24	19.21	21.54	23.43	21.25	21.00	22.26
Emu 2 [54]	29.49	26.21	23.67	20.85	19.56	26.09	20.53	19.81	24.25
DreamLLM [54]	27.16	23.47	25.57	25.13	24.27	23.31	20.78	24.20	23.98
SEED-LLaMA [14]	27.18	23.97	16.73	19.66	19.03	22.66	19.63	19.29	22.00
LaVIT [20]	34.60	29.07	16.70	25.17	24.14	29.59	25.07	24.26	27.07
SEED-LLaMA (Ours)	27.16	23.47	25.57	25.13	24.27	23.31	20.78	24.20	23.98
LaVIT (Ours)	32.05	25.39	35.87	24.30	32.38	31.28	27.59	31.01	28.45

Table 7: Unified performance comparison on the *CLIP-I score* across 8 domains in TIGeR-Bench.

Method	Creative Domains		Logo	News	Knowledge Domains		Food	Wiki	All
	Counterfactual	Preference			Landmark	Nature			
SDXL [43]	65.91	55.38	14.21	42.09	35.43	44.94	45.60	35.40	46.71
CLIP (ViT-B/32) [46]	31.33	26.68	93.55	91.04	71.54	75.38	71.39	75.59	53.60
GILL [24]	15.93	13.61	20.38	15.96	14.34	18.25	15.49	14.52	15.25
Emu [55]	43.17	43.95	22.23	34.25	38.53	46.97	48.56	35.97	40.78
Emu 2 [54]	59.07	49.17	32.27	36.27	33.44	49.77	40.72	33.51	44.24
DreamLLM [54]	53.93	46.22	33.16	32.09	37.87	46.06	43.82	35.13	42.77
SEED-LLaMA [14]	52.76	49.37	18.50	37.89	33.78	45.46	46.55	34.50	43.02
LaVIT [20]	65.79	53.64	20.87	42.20	39.77	53.66	52.48	42.05	48.75
SEED-LLaMA (Ours)	52.67	47.81	51.94	56.86	48.76	51.99	52.53	52.52	50.52
LaVIT (Ours)	60.80	46.56	92.68	57.32	72.88	74.70	69.79	75.44	61.37

between images and tokens. Based on these discrete tokens, we construct a Trie for efficient storage and constrained generation. The beam size for retrieval is set to 800, and the timestep for generation is 25.

D Additional Experiments

In this section, we carry out extensive experiments and obtain quantitative and qualitative results to explore the unified text-to-image generation and retrieval problem and the proposed MLLMs-based method.

D.1 Additional Quantitative Results

D.1.1 Unified Performance Comparison

To broadly compare the performance of baselines and our method for unified text-to-image generation and retrieval, we report the results with the CLIP-T score and the CLIP-I score as the evaluation metrics across 8 domains in TIGeR-Bench, in Tab. 6 and Tab. 7, respective.

D.1.2 Prompt/Query Extension

In this section, we mainly study the influence of prompts on the retrieval and generation performance in knowledge-intensive scenarios. Toward this end, we first let SEED-LLaMA, Gemini Pro, and GPT-4o to explain the raw query with knowledge concepts from 6 domains. Subsequently, we concatenate the raw prompt and expanded ones to form new long text prompts and feed them to SEED-LLaMA. The results for text-to-image generation and retrieval are listed in Tab. 8 and Tab. 9, respectively. We can see that prompt/query expansion with strong LLMs could promote both generation and retrieval performance. Meanwhile, weak LLMs may introduce false explanations and do harm to the generation and retrieval performance.

Besides, we also investigate the generation and retrieval performance separately in multi-round chat scenarios. To construct such scenarios, we use the APIs of powerful Gemini Pro and GPT-4o to imagine chat contexts and then feed the context into SEED-LLaMA. Experimental results on these two tasks are reported in Tab. 10.

Table 8: Text-to-image *generation* performance on TIGeR-Bench (Knowledge) in *long text* scenarios, with CLIP-T and CLIP-I scores as evaluation metrics across various prompt/query expansion methods including Self-Expansion, Gemini Pro, and GPT-4o. For expansion, we guide LLMs to explain the appearance characteristics in detail with their expert language knowledge for given raw queries by giving them detailed instructions. After that, the queries can be expanded into longer texts and are combined with raw queries as input for text-to-image generation. We perform generative retrieval with 200 beams.

Expansion Method	Ours (SEED-LLaMA)		Ours (LaVIT)	
	CLIP-T	CLIP-I	CLIP-T	CLIP-I
Raw Query	19.50	36.11	24.16	41.84
Self-Expansion	18.07	35.12	-	-
Gemini-Pro	17.48	34.74	22.38	39.28
GPT-4o	20.36	38.95	23.91	42.59

Table 9: Text-to-image *retrieval* performance on TIGeR-Bench (Knowledge) in *long text* scenarios, with recall as the evaluation metric across various prompt/query expansion methods including Self-Expansion, Gemini Pro, and GPT-4o. For expansion, we guide LLMs to explain the appearance characteristics in detail with their expert language knowledge for given raw queries by giving them detailed instructions. After that, the queries can be expanded into longer texts and are combined with raw queries as input for text-to-image retrieval. We perform generative retrieval with 200 beams.

Expansion Method	Ours (SEED-LLaMA)			Ours (LaVIT)		
	R@1	R@5	R@10	R@1	R@5	R@10
Raw Query	22.57	36.80	43.23	25.63	43.63	49.40
Self-Expansion	17.20	30.10	36.77	-	-	-
Gemini-Pro	18.57	34.27	40.30	19.07	36.80	43.10
GPT-4o	25.00	42.50	48.90	25.20	46.03	52.17

Table 10: Text-to-image generation and retrieval performance on TIGeR-Bench (Knowledge) in *chat* scenarios, across various chat generation methods including Gemini Pro and GPT-4o. We guide LLMs to imagine a scenario where a user intends to know a concept and asks for an image with their expert language knowledge for given raw queries by giving them detailed instructions and in-context examples. After that, the queries can be expanded into multi-round chat contexts as input for text-to-image generation and retrieval. Considering that LaVIT was not fine-tuned by chat instructions, we only carry out experiments based on SEED-LLaMA. We perform generative retrieval with 200 beams.

Expansion Method	Text-to-Image Generation		Text-to-Image Retrieval		
	CLIP-T	CLIP-I	R@1	R@5	R@10
Raw Query	19.50	36.11	22.57	36.80	43.23
Gemini-Pro	17.71	34.58	17.83	31.70	36.77
GPT-4o	19.40	38.17	24.03	40.73	47.83

We also carry out experiments in multimodal chat scenarios to explore the interplay between generation and retrieval, as shown in 11. Specifically, we concatenate the retrieved top-1 images behind the chat context and then evaluate the generation performance. Similarly, we concatenate the generated images behind the chat context and then evaluate the retrieval performance.

D.1.3 Ablation Study

In this part, we conduct comprehensive ablation studies on the components of the proposed method to study the effectiveness.

First, we compare the alignment performance between separate generation, retrieval, and unified variants across all 8 domains. The results are listed in Tab. 12 and Tab. 13 with the CLIP-T and CLIP-I score as the evaluation protocols, respectively. Besides, although Flickr30K and MS-COCO are the general datasets describing daily common scenes, we also investigate the three variants on them, as shown in Tab. 14

Table 11: Text-to-image generation and retrieval performance on TIGeR-Bench (Knowledge) in *multimodal chat* scenarios. Based on the chat contexts with pure text generated by GPT-4o, we can perform generation and retrieval. Afterwards, we concatenate the generated or retrieved top-1 images with the chat contexts and form the multimodal context, to explore the influence on retrieval and generation, respectively. Considering that LaVIT was not fine-tuned by chat instructions, we only carry out experiments based on SEED-LLaMA. We perform generative retrieval with 200 beams.

Expansion Method	Image Context	Text-to-Image Generation		Text-to-Image Retrieval		
		CLIP-T	CLIP-I	R@1	R@5	R@10
Raw Query	-	19.50	36.11	22.57	36.80	43.23
GPT-4o	Retrieved	18.62	38.20	-	-	-
GPT-4o	Generated	-	-	15.87	29.13	35.60

Table 12: Comparison of *CLIP-T score* between the unified method and single generation and retrieval variants based on SEED-LLaMA and LaVIT on 8 domains of TIGeR.

Method	Creative Domains		Knowledge Domains						All
	Counterfactual	Preference	Logo	News	Landmark	Nature	Food	Wiki	
<i>Ours (SEED-LLaMA)</i>									
Generation	27.18	23.97	16.73	19.66	19.03	22.66	19.63	19.29	22.00
Retrieval	11.04	10.36	27.87	26.21	23.73	20.25	19.56	22.99	16.95
Unified	27.16	23.47	25.57	25.13	24.27	23.31	20.78	24.20	23.98
<i>Ours (LaVIT)</i>									
Generation	34.60	29.07	16.70	25.17	24.14	29.59	25.07	24.26	27.07
Retrieval	13.21	12.17	35.84	23.64	32.58	31.08	27.61	30.76	21.30
Unified	32.05	25.39	35.87	24.30	32.38	31.28	27.59	31.01	28.45

Table 13: Comparison of *CLIP-I score* between the unified method and single generation and retrieval variants based on SEED-LLaMA and LaVIT on 8 domains of TIGeR-Bench.

Method	Creative Domains		Knowledge Domains						All
	Counterfactual	Preference	Logo	News	Landmark	Nature	Food	Wiki	
<i>Ours (SEED-LLaMA)</i>									
Generation	27.18	23.97	16.73	19.66	19.03	22.66	19.63	19.29	22.00
Retrieval	11.04	10.36	27.87	26.21	23.73	20.25	19.56	22.99	16.95
Unified	27.16	23.47	25.57	25.13	24.27	23.31	20.78	24.20	23.98
<i>Ours (LaVIT)</i>									
Generation	34.60	29.07	16.70	25.17	24.14	29.59	25.07	24.26	27.07
Retrieval	13.21	12.17	35.84	23.64	32.58	31.08	27.61	30.76	21.30
Unified	32.05	25.39	35.87	24.30	32.38	31.28	27.59	31.01	28.45

Table 14: Comparison between the unified method and single generation and retrieval variants based on SEED-LLaMA and LaVIT on the Flickr30K and MS-COCO datasets. Performance is evaluated by the CLIP-T score.

Method	Flickr30K	MS-COCO
<i>Ours (SEED-LLaMA)</i>		
Generation	28.65	27.74
Retrieval	29.86	28.73
Unified	30.01	29.09
<i>Ours (LaVIT)</i>		
Generation	37.05	35.59
Retrieval	27.54	27.13
Unified	33.69	32.24

Second, we further study the effects of the directions of re-ranking and decision-making, across 8 domains in Tab. 15, and 2 general datasets, *i.e.*, Flickr30K and MS-COCO, in Tab. 16.

In addition, we delve into the discriminative abilities by forward and reverse ranking methods, as well as forward beam search and reverse re-ranking in Tab. 17 on 6 knowledge-intensive domains.

Table 15: Ablation study on 8 domains of TIGeR-Bench investigating Reverse Re-Ranking (RRR) and two decision-making strategies, *i.e.*, Forward with Eqn. 3 and Reverse with Eqn. 4. Performance is evaluated by the *CLIP-T score*.

RRR	Decision	Creative Domains		Logo	News	Knowledge Domains		Food	Wiki	All
		Counterfactual	Preference			Landmark	Nature			
<i>Ours (SEED-LLaMA)</i>										
✓	Forward	26.64	22.41	24.02	23.64	22.85	20.34	19.63	22.40	22.63
	Forward	27.14	23.95	23.57	23.18	22.82	24.57	20.62	22.93	23.72
✓	Reverse	27.16	23.47	25.57	25.13	24.27	23.31	20.78	24.20	23.98
	Reverse	26.81	20.19	27.29	23.22	24.16	26.04	21.79	23.84	22.84
<i>Ours (LaVIT)</i>										
✓	Forward	34.59	29.00	16.84	25.53	24.74	29.56	24.93	25.05	27.19
	Forward	32.05	29.07	17.15	25.57	24.76	29.60	25.17	25.20	27.28
✓	Reverse	33.83	28.17	24.67	28.88	28.06	29.02	25.65	27.84	28.23
	Reverse	32.05	25.39	35.87	24.30	32.38	31.28	27.59	31.01	28.45

Table 16: Ablation study on Flickr30K and MSCOCO investigating Reverse Re-Ranking (RRR) and two decision-making strategies, *i.e.*, Forward with Eqn. 3 and Reverse with Eqn. 4. %Retr. denotes the percentage of retrieved images selected as results.

RRR	Decision	Flickr30K			MS-COCO		
		CLIP-T ↑	R@1 ↑	%Retr.	CLIP-T ↑	R@1 ↑	%Retr.
<i>Ours (SEED-LLaMA)</i>							
✓	Forward	28.89	58.50	39.52	25.95	26.17	67.61
	Forward	29.68	71.70	26.92	28.71	46.11	33.91
✓	Reverse	30.01	58.50	35.98	28.61	26.17	26.23
	Reverse	30.02	71.70	51.88	29.09	46.11	60.69
<i>Ours (LaVIT)</i>							
✓	Forward	37.03	47.86	0.20	35.34	23.20	3.44
	Forward	37.04	68.84	0.10	35.58	44.81	0.23
✓	Reverse	36.18	47.86	24.34	34.67	23.20	20.60
	Reverse	33.69	68.84	41.84	32.24	44.81	49.11

Table 17: Recall@1 performance comparison of Forward Ranking, Reverse Ranking, Forward Beam Search (FBS) with different beam sizes, and BFS + Reverse Re-Ranking (RRR). Experiments are conducted based on SEED-LLaMA and LaVIT on 6 knowledge-intensive domains of TIGeR-Bench.

Method	Logo	News	Landmark	Nature	Food	Wiki	ALL
<i>Ours (SEED-LLaMA)</i>							
Forward Ranking	56.00	45.60	22.60	2.60	4.40	30.40	26.93
Reverse Ranking	61.80	40.40	26.60	15.00	7.00	32.40	30.53
FBS (#Beam=100)	39.40	29.60	10.40	8.80	4.60	19.40	18.70
FBS (#Beam=800)	56.00	46.80	20.20	3.60	4.60	29.60	26.80
FBS (#Beam=100) + RRR	37.40	25.80	10.00	10.20	6.00	18.60	18.00
FBS (#Beam=800) + RRR	61.20	39.60	22.60	15.40	6.80	29.80	29.23
<i>Ours (LaVIT)</i>							
Forward Ranking	37.80	52.20	25.00	10.00	11.40	33.20	28.27
Reverse Ranking	92.20	41.00	56.00	36.40	23.60	63.80	52.17
FBS (#Beam=100)	16.60	46.00	20.20	9.40	10.00	28.40	21.77
FBS (#Beam=800)	37.00	53.40	24.40	10.80	11.40	31.80	28.13
FBS (#Beam=100) + RRR	27.00	30.80	30.60	16.80	15.40	41.00	26.93
FBS (#Beam=800) + RRR	87.20	40.40	51.60	34.60	23.00	59.40	49.37

D.2 Additional Qualitative Results

We showcase more examples of our SEED-LLaMA and LaVIT in both creative and knowledge-intensive domains in Fig. 8 and Fig. 9.

In the creative domain, the CLIP model, limited to retrieving images from the database, shows significant discrepancies when compared to the ground truth images. Our SEED-LLaMA and LaVIT, capable of both generation and retrieval, tend to favor image generation in the creative domain.

However, our models also exhibit decision errors. For instance, as demonstrated in the last two rows of Fig. 8, the models incorrectly selected misleading retrieved images.

As shown in Fig. 8, our models has the advantages over SDXL in the knowledge-intensive domain, accurately retrieving the correct results. However, decision errors still occur. We leave further exploration of the decision strategy for future work.

In Fig. 10, we compare our models with current Text-to-Image baseline models such as Emu2, DreamLLM, and GILL, which can autonomously decide between retrieval and generation. Our models are consistently retrieving the correct images in the knowledge-intensive domain. In this domain, Emu2, DreamLLM, and GILL fail to generate closely matching images, highlighting the limitations of current MLLMs.

We further explored two scenarios: Augmented Generation for Better Retrieval and Augmented Retrieval for Better Generation. In the Augmented Generation for Better Retrieval scenario, we first use the MLLM’s capability to generate an image before performing image retrieval. The generated image, along with the retrieval prompt, is then used as input for the retrieval process. As shown in Fig. 11, generating an image beforehand improves the model’s retrieval performance.

In the Augmented Retrieval for Better Generation scenario, we leverage our model’s generative retrieval capabilities to perform an image retrieval before generating an image. The retrieved image, along with the generation prompt, is then used as input for the generation process, similar to Retrieval-Augmented Generation (RAG). As shown in Fig. 12, performing image retrieval beforehand improves the stability and quality of the generated images.

One major limitation of the CLIP model for retrieval is its limited context length. Our model leverages the advantage of the LLM’s long context length, making retrieve with longer prompts possible. As shown in Fig. 13, extending the prompt further enhances the retrieval performance of our model.

E Future Work

In the future, we plan to investigate the root causes of modality biases from various perspectives, including data distribution, model architecture, and optimization objectives. We will also examine the potential impacts of these biases on generative and discriminative tasks. Additionally, we aim to study more complex contexts involving interleaved multimodal content to advance comprehensive unified generation and retrieval tasks. Finally, it would be valuable to explore the deeper relationships and possible interactions between generation and retrieval (e.g., retrieval-augmented generation and generation-augmented retrieval) within the TIGeR framework.

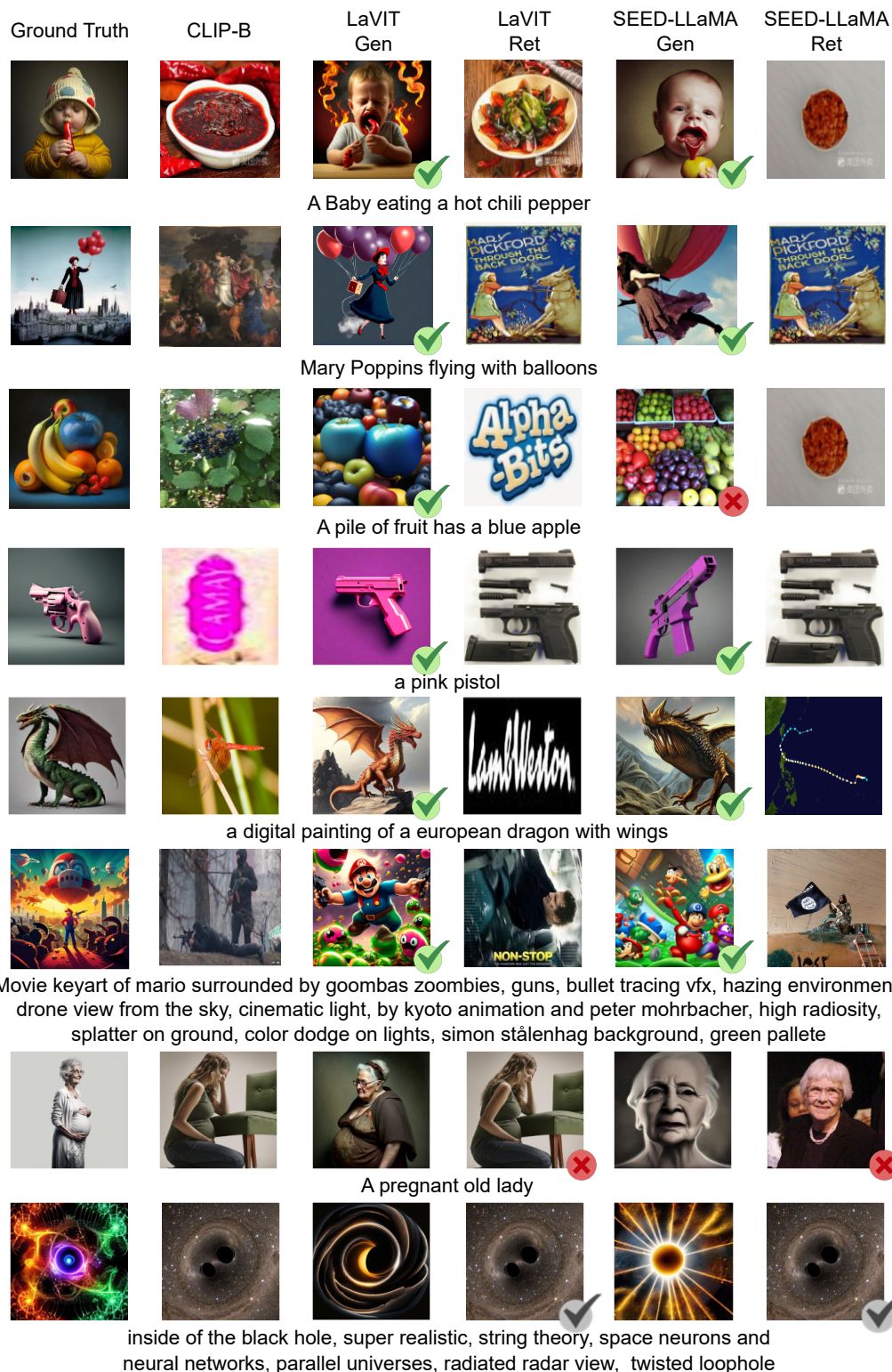
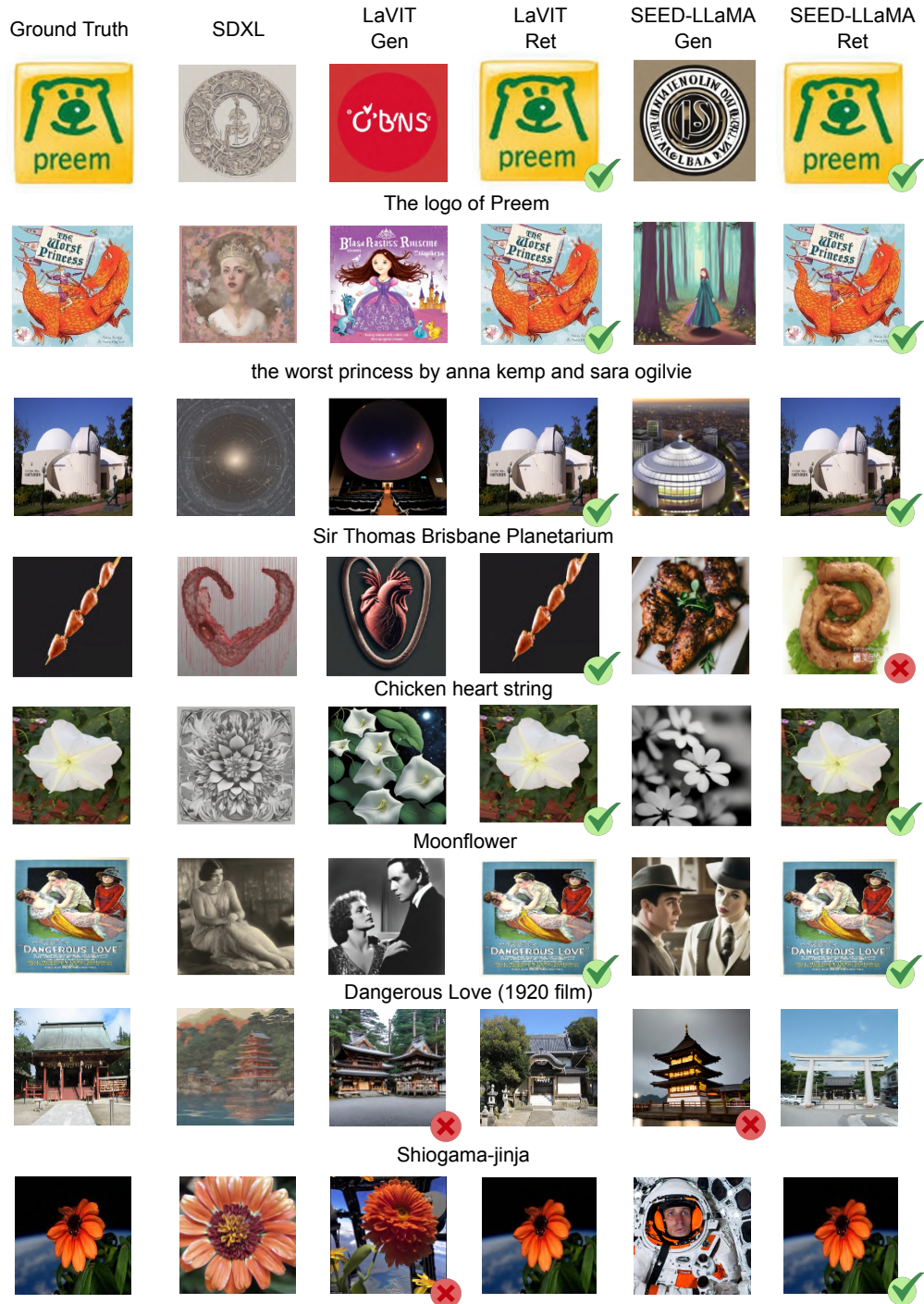


Figure 8: Qualitative results in TIGeR-Bench creative domain. We use ticks or crosses to highlight the selected results from generation or retrieval. Green ticks indicate the correct generated images and red crosses indicate the wrong retrieved images. Black ticks refer to the correct retrieved images despite the creative domain.



international space stationa bright orange zinnia has blossomed aboard the international space station marking a first in space us astronaut scott kelly who took the photograph tweeted first flower ever grown in space makes its debut zinnias grow easily on earth and blossom in abundance in summer but on the iss they have had trouble adapting to microgravity

Figure 9: Qualitative results in TIGeR-Bench knowledge domain. We use ticks or crosses to highlight the selected results from generation or retrieval. Green ticks indicate the correct retrieved images and red crosses indicate the wrong generated images.

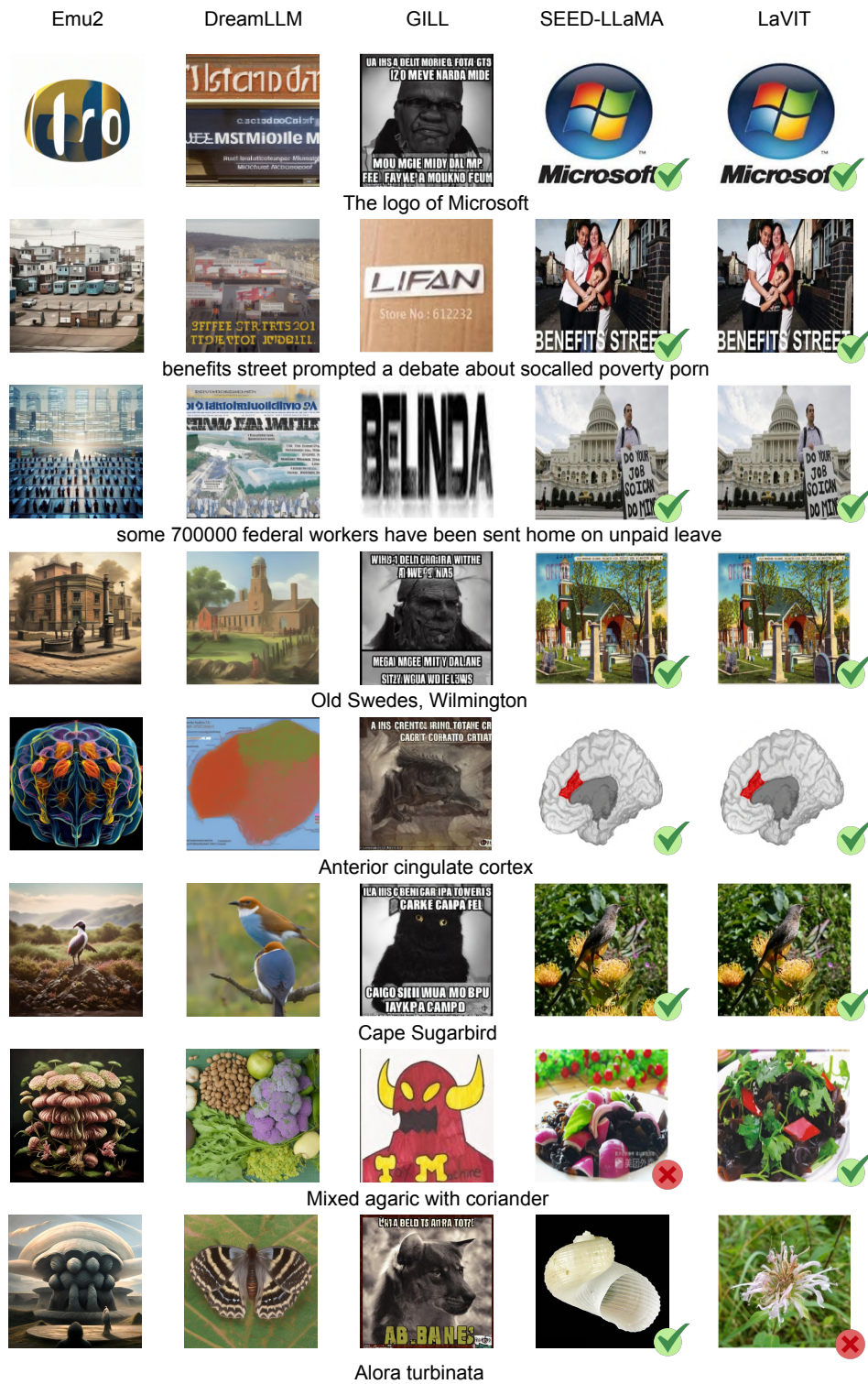


Figure 10: Qualitative results in TIGer-Bench knowledge domain compared to Text-to-Image generation baselines. Green tick indicates the final output by our model is correct and Red cross indicates the final output by our model is incorrect.

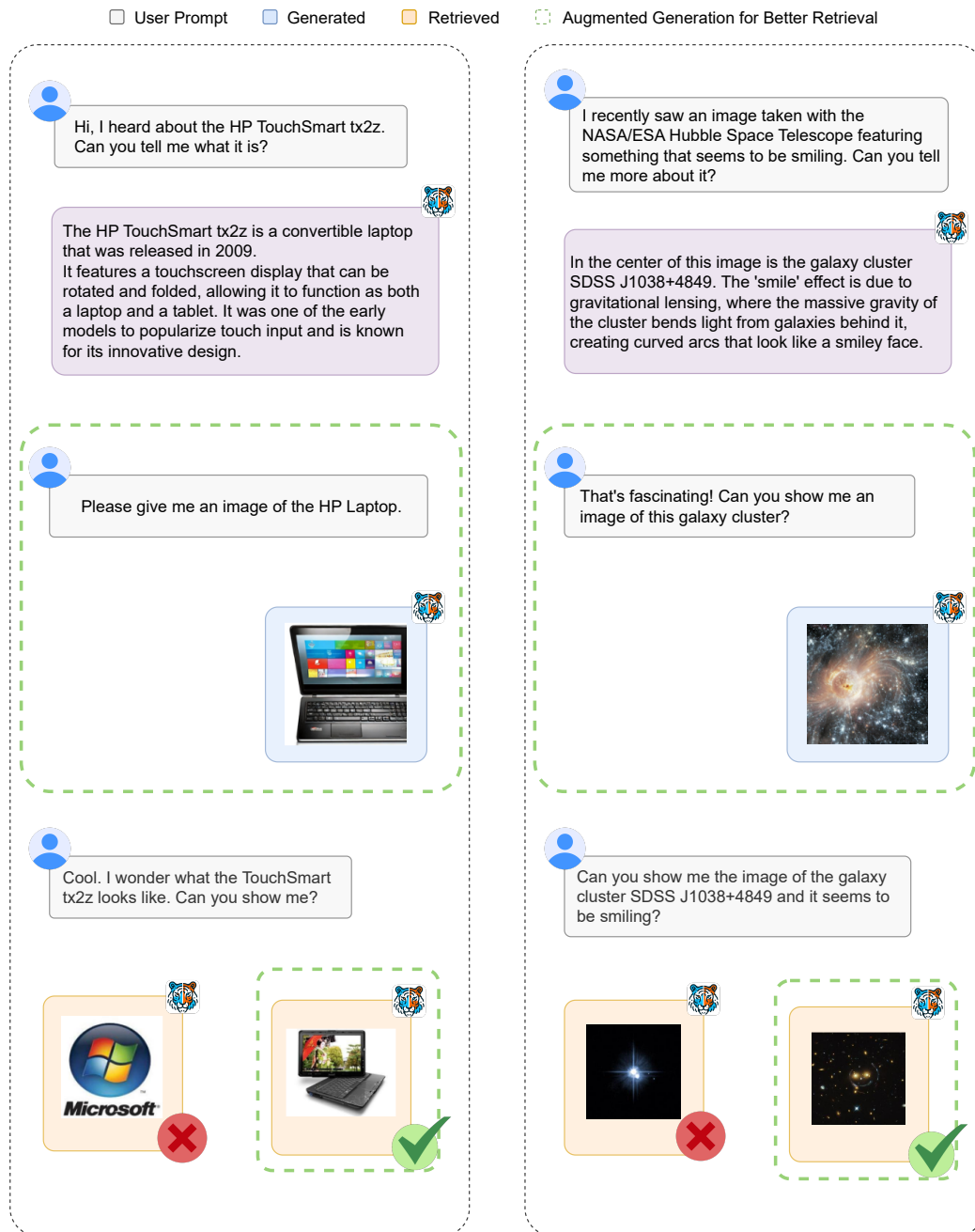


Figure 11: Augmented generation for better retrieval. Green box is the additional generation step. Green tick indicates the final output by our model is correct and Red cross indicates the final output by our model is incorrect.

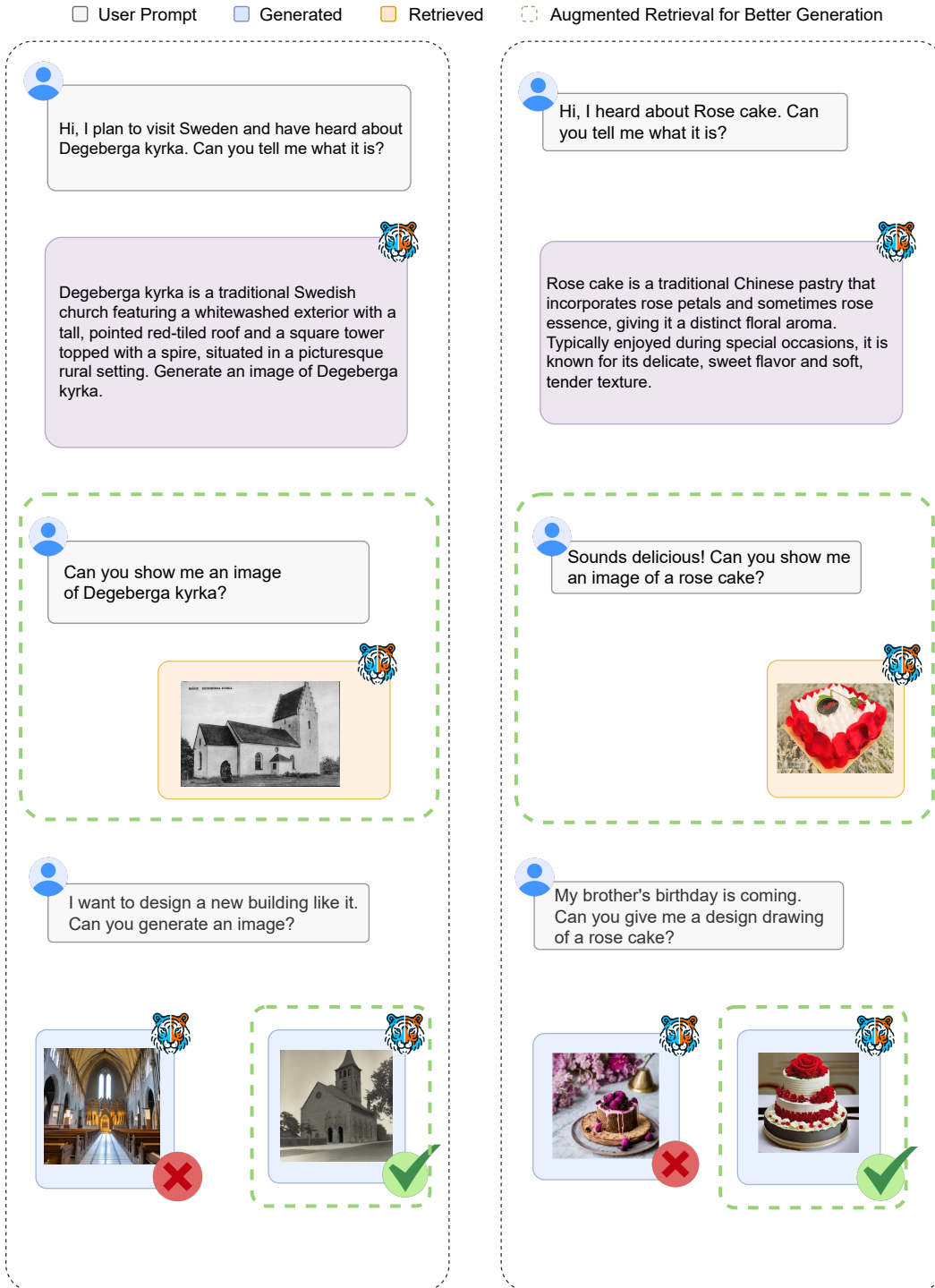


Figure 12: Augmented retrieval for better generation. Green box is the additional retrieval step. Green tick indicates the final output by our model is consistent and Red cross indicates the final output by our model is inconsistent.

Short Prompt Retrieval Long Prompt Retrieval

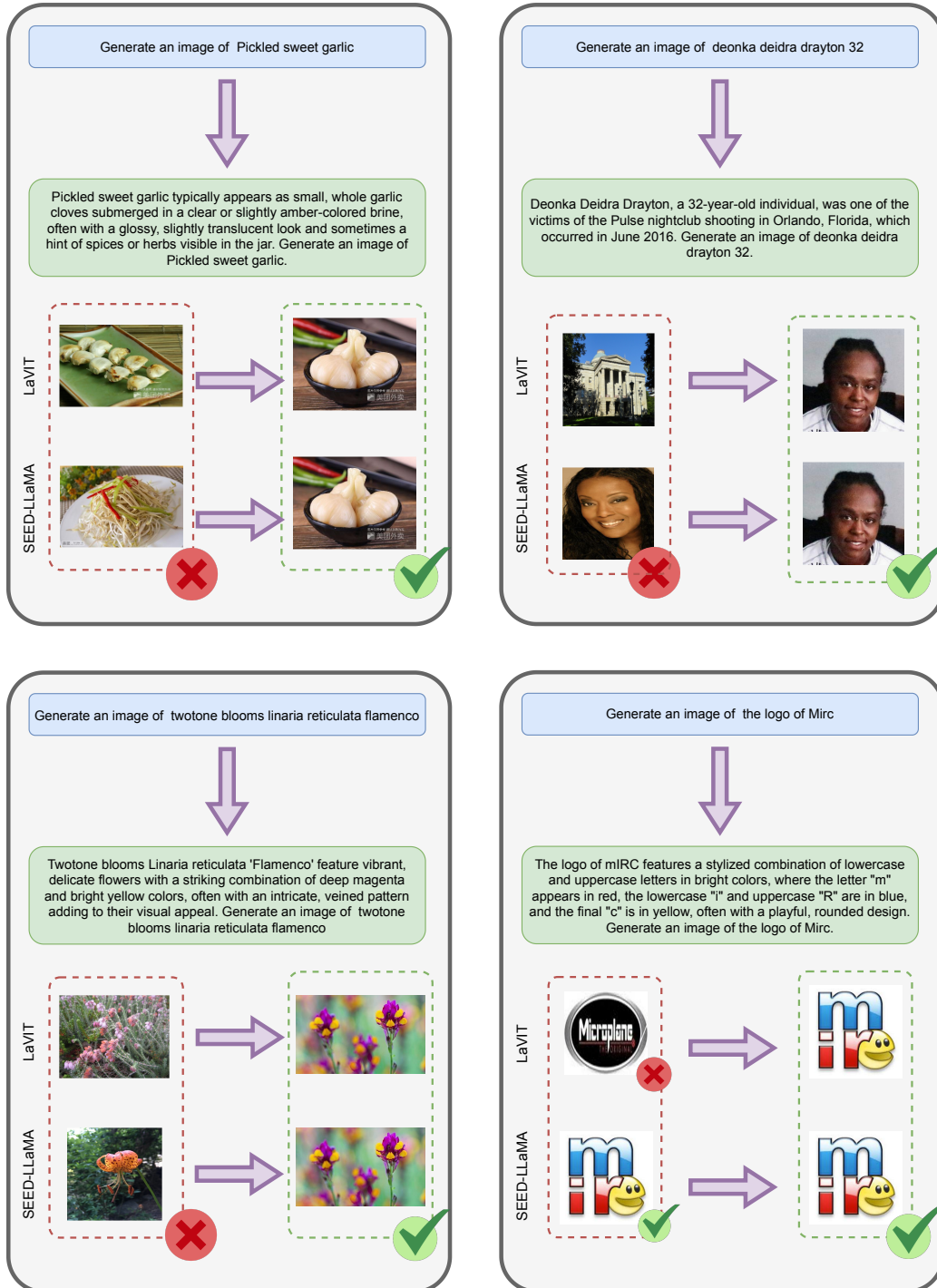


Figure 13: Short prompt and long prompt retrieval comparison on TIGeR-Bench knowledge domain. Red box is the retrieve result of short prompt. Green box is the retrieve result of long prompt. Green tick indicates the final output by our model is correct and Red cross indicates the final output by our model is incorrect.